Matrix cross-linking lysyl oxidases are induced in response to myocardial infarction and promote cardiac dysfunction

José González-Santamaría[1], María Villalba[2], Oscar Busnadiego[1], Marina M. López-Olañeta[2], Pilar Sandoval[1], Jessica Snabel[3], Manuel López-Cabrera[1], Janine T. Erler[4], Roeland Hanemaaijer[3], Enrique Lara-Pezzi[2*] and Fernando Rodríguez-Pascual[1*]

[1]Centro de Biología Molecular "Severo Ochoa", Consejo Superior de Investigaciones Científicas (C.S.I.C.), Universidad Autónoma de Madrid (U.A.M.), Madrid, Spain.
[2]Cardiovascular Development and Repair Department, Centro Nacional de Investigaciones Cardiovasculares (C.N.I.C.), Madrid, Spain.
[3]TNO Metabolic Health Research, Leiden, The Netherlands.
[4]Biotech Research & Innovation Centre (BRIC), University of Copenhagen (UCPH), Denmark.

*Enrique Lara-Pezzi and Fernando Rodríguez-Pascual contributed equally to this work.

Address correspondence to:

Dr. Fernando Rodríguez-Pascual Centro de Biología Molecular "Severo Ochoa", Consejo Superior de Investigaciones Científicas (C.S.I.C.), Universidad Autónoma de Madrid (U.A.M.). Nicolás Cabrera 1. Madrid, E28049 Spain Phone: 34 91 196 4505 Fax: 34 91 196 4420 Email: frodriguez@cbm.csic.es	Dr. Enrique Lara-Pezzi Cardiovascular Development and Repair Department, Centro Nacional de Investigaciones Cardiovasculares (C.N.I.C.). Melchor Fernandez Almagro 3. Madrid, E28029 Spain. Phone: 34 91 453 3309 Fax: 34 91 453 1245 Email: elara@cnic.es

Total word count of the manuscript (including the abstract, manuscript text, references, and figure legends): 6942

Short title: Lysyl Oxidases and Myocardial Infarction

Abstract

Aims: After myocardial infarction (MI), extensive remodeling of extracellular matrix contributes to scar formation. While aiming to preserve tissue integrity, this fibrotic response is also associated with adverse events, including a markedly increased risk of heart failure, ventricular arrhythmias and sudden cardiac death. Cardiac fibrosis is characterized by extensive deposition of collagen, but also by increased stiffness as a consequence of enhanced collagen cross-linking. Members of the lysyl oxidase (LOX) family of enzymes are responsible for the formation of collagen cross-links. The present study investigates the contribution of LOX family members to the heart response to myocardial infarction.

Methods and Results: Experimental MI was induced in C57BL/6 mice by permanent ligation of the left anterior descending coronary artery. The expression of LOX isoforms (LOX and LOXL1 to 4) was strongly increased upon MI, and this response was accompanied by a significant accumulation of mature collagen fibers in the infarcted area. LOX expression was observed in areas of extensive remodeling, partially overlapping with α-smooth muscle actin (α-SMA)-expressing myofibroblasts. TGF-β- as well as hypoxia-activated pathways contributed to the induction of LOX expression in cardiac fibroblasts. Finally, *in vivo* post-infarction treatment with the broad band LOX inhibitor β-aminopropionitrile (BAPN) or, selectively, with a neutralizing antibody against the canonical LOX isoform attenuated collagen accumulation and maturation, and also resulted in reduced ventricular dilatation and improved cardiac function.

Conclusions: LOX family members contribute significantly to the detrimental effects of cardiac remodeling, highlighting LOX inhibition as a potential therapeutic strategy for post-infarction recovery.

Keywords

Myocardial infarction, cardiac fibrosis, lysyl oxidases, collagen, myofibroblast.

Non-standard Abbreviations and Acronyms

ALK5: activin-like kinase 5.
α-SMA: α-smooth muscle actin.
BAPN: β-aminopropionitrile.
cTNI: cardiac troponin I.
DAPI: 4',6-diamidino-2-phenylindole.
ECM: extracellular matrix.
HIF1α: hypoxia-induced factor-1α.
HP: hydroxylysylpyridinoline.
HPLC: high performance liquid chromatography.
LOX: lysyl oxidase.
LOXL: lysyl oxidase-like.
LP: lysylpyridinoline.
LV: left ventricule.
LVESD: left ventricular end-systolic diameter.
LVEDD: left ventricular end-diastolic diameter.
MI: myocardial infarction.
RT-PCR: reverse-transcribed polymerase chain reaction.
SHR: spontaneous hypertensive rat.
TGF-β: transforming growth factor-β.

Introduction

Extensive remodeling of the cardiac extracellular matrix (ECM) occurs during myocardial infarction. As an orchestrated response to heart damage, loss of myocardial mass due to ischemia induces cardiac fibrosis, mainly, but not only, mediated by the transdifferentiation of fibroblasts to myofibroblasts, with significant collagen production and deposition[1]. Since adult mammals have a limited capacity to regenerate the cardiomyocytes after cell death, this "reparative" fibrotic response constitutes the only way for the entire organ to preserve its structural integrity, avoid rupture and maintain its pumping capacity. However, this progressively leads to cardiac remodeling, increased tissue stiffness and propensity to arrhythmias and eventually to heart failure.

Collagen is a relatively stiff material with a high tensile strength; therefore tissue stiffness is expected to increase upon collagen deposition following a MI. However, recent studies have shown that increased collagen production and deposition in itself is not always directly translated into increased stiffness, and that myocardial damage results not only in an increase in collagen content but also in structural qualitative changes in collagen network[2, 3]. One of the characteristic features of collagen is its extensive post-translational modifications, including proline and lysine hydroxylation, glycosylation of specific hydroxylysine residues, oxidative deamination of the ε-amino groups of peptidyl lysine/hydroxylysine in the telopeptide domains of the molecule, and subsequent intra/intermolecular covalent cross-linking [4]. Collagen tensile strength importantly relies on cross-linking [5]. This has led to the proposal that it is not only the amount of collagen that matters; it is the cross-linking which determines the stiffness. In fact, enhanced collagen cross-linking has been observed in the failing human heart, and it has been further demonstrated that it is the degree of cross-linking that significantly correlates with chamber stiffness[6, 7]. The members of the lysyl oxidase (LOX) family are responsible for initiating covalent cross-linking formation by catalyzing the oxidative deamination of lysine/hydroxylysine residues in collagen telopeptide domains, a process progressing into non-enzymatically condensation of aldehyde groups to form the mature cross-links. Five different LOX enzymes have been identified in mammals, the canonical LOX, and four LOX-like isoforms, LOXL1-4[8]. Abnormally increased expression of the active form of LOX and of LOX mRNA has been reported in the fibrotic myocardium of patients with heart disease[9]. LOX mRNA and protein have been also found to be upregulated in animal models of heart failure, including MI, together with a significant increase in collagen cross-linking and chamber stiffness[10, 11].

Based on these clinical and experimental observations, it is conceivable that LOX upregulation may play a significant role in cardiac remodeling upon MI. Nevertheless, the specific contribution of the LOX family members in the response to MI and whether they play beneficial or detrimental roles during heart remodeling is virtually unknown. In this work, we aimed to assess the expression of LOX isoforms in a mouse model of MI, as well as to analyze the main cell type/s responsible for their expression. Finally, we studied the contribution of this family of enzymes to cardiac remodeling and function, as an obligate step in their validation as pharmacological target for post-MI treatment.

Methods

A detailed description of the methods is provided in **Supplementary material online**.

Mouse model of myocardial infarction

MI was induced in C57BL/6 by permanently ligating the left coronary artery as previously described[12]. Control, uninfarcted animals were sham-operated.

Cardiac function, chamber dilatation, and wall thickness were analyzed by transthoracic echocardiography 3 and 28 days after infarction, as well as in uninfarcted mice, using a Vevo 2100 high resolution ultrasound system equipped with a 30-MHz linear array transducer (Visualsonics, Toronto, Canada). For LOX inhibition studies, mice were treated either with β-aminopropionitrile (BAPN, 5 mg/kg body weight/day; Sigma-Aldrich, St. Louis, Missouri) (n=10 per group) or with a rabbit polyclonal antibody reported to specifically block LOX isoform (1 mg/kg body weight/twice weekly), injected intraperitoneally (n=5 per group) [13]. Control mice received PBS as vehicle for BAPN, or the same amount of control IgG (Sigma-Aldrich) for anti-LOX. In two experimental groups, BAPN treatment started either on the same day or eight days after MI. The administration of anti-LOX antibody was initiated eight days after MI. Both animal trials were ended at day 28 post-infarction. Animals were sacrificed by gradually filling the chamber with carbon dioxide.

The investigation conforms to the principles of Laboratory Animal Care, which are formulated by the National Society for Medical Research and the Guide for the Care and Use of Laboratory Animals (US National Institutes of Health, 2011), and the Directive 2010/63/EU of the European Parliament on the protection of animals used for scientific purposes.

Histological and immunohistochemical studies

The extent of cardiac damage and fibrosis was assessed by standard histological and immunohistochemical methodologies. Immunohistochemical stainings and double immunofluorescence were performed using methods previously described [14].

RNA extraction and quantitative real-time reverse-transcribed polymerase chain reaction

For RNA studies, heart tissue was snap-frozen in liquid nitrogen. Total RNA was extracted using the RNAeasy kit (Qiagen), the cDNA was synthesized (iScript cDNA synthesis kit, Bio-Rad, Hercules, California) and quantitative real time reverse-transcribed polymerase chain reaction (RT-PCR) was performed as described with off-the-shelf Taqman probes (Applied Biosystems, Foster City, California) [12].

Collagen and collagen cross-linking analysis

Heart tissue portions were hydrolyzed (110°C, 24 hours) in 6 M HCl and collagen (hydroxyproline and proline) and mature trivalent cross-links, hydroxylysylpyridinoline (HP) and lysylpyridinoline (LP), analyzed as described previously [15].

Culture of cardiac fibroblasts

Mice were sacrificed by gradually filling the chamber with carbon dioxide and cardiac fibroblasts were isolated from 8-week old mouse heart tissue using methods previously described [16]. Mouse cardiac fibroblasts were treated for time periods ranging from 8 to 48 hours with TGF-β1 at 5 ng/ml under normoxic or hypoxic conditions (1% O_2 tension,

Hypoxystation H35, Don Whitley, Shipley, England). At the end of the experimental period, total RNA or protein were extracted and analyzed following protocols previously described[14].

Statistical Analysis

Data are presented as mean ± SE. In echocardiographic data, the same mice were analyzed 3 and 28 days post-infarction, with non-infarcted animals representing a different group of mice. To test for statistical significance, data were analyzed by one- or two-way ANOVA followed by Bonferroni post-test, or by unpaired t-test as indicated in the corresponding table and figure legends. Statistics was performed with GraphPad Prism 5.0 (La Jolla, California), and differences were considered statistically significant at $P< 0.05$.

Results

Increased LOX and LOXL expression after MI

In order to gain insight about the potential contribution of LOX family members to the heart response to MI, we established an infarct mouse model with permanent ligation of the left anterior descending artery. Cross-sections of the ventricles stained with Picrosirius red and visualized under brightfield light microscopy showed that coronary artery ligation resulted in large transmural infarcts with progressive accumulation of collagen and left ventricular wall thinning in the infarct area **(Supp. Fig. 1A-C)**. Interestingly, collagen visualization by Picrosirius red staining under polarized light showed long and highly aligned collagen fibers in the remodeled heart of mice at 7-28 days post injury, in marked contrast to mice with no infarct or those sacrificed 3 days after coronary ligation, which displayed an almost black background **(Fig. 1A)**. Quantification of immature (greenish-yellow) and mature (reddish-orange) collagen revealed a progressive accumulation of mature fibers when compared to immature collagen **(Fig. 1B)**. While the presence of highly birefringent collagen scaffolds does not directly demonstrate enhanced cross-linking, these observations indicate the potential involvement of LOX upregulation in the formation of mature collagen bundles in the fibrotic scar of the infarcted heart. In order to analyze the expression profile of LOX family members in response to MI, three heart regions were defined corresponding to the scar (infarct), the peri-infarct (border), and the sites distant from the infarct area (remote), as indicated in the micrograph taken 28 days post injury (Supp. Fig. 1A). Total RNA was extracted from these regions and analyzed by real time quantitative RT-PCR. Compared with uninjured hearts, MI induced increases in the expression of the whole set of LOX genes in all areas studied, with higher induction rates in the infarct, diminishing gradually in border and remote zones **(Fig. 1C)**. Gene expression increases were detectable at 3 days post injury and peaked between 3-7 days for all of the isoforms. These results were confirmed by immunohistochemical analysis for LOX, LOXL2 and LOXL4 at 7 days after coronary ligation as compared with control **(Fig. 2A, 2B)**. Available antibodies for LOXL1 and LOXL3 did not work in our hands (data not shown).

Myofibroblasts dominate the regulation of collagen turnover in the injured heart[1]. In order to study whether myofibroblasts are the main source for the expression of LOX after myocardial infarction, consecutive cross-sections of control and infarcted hearts (7 days post-MI) were analyzed for the expression of the canonical LOX, the most highly induced LOX isoform in our experimental conditions, and of the myofibroblast marker α-smooth muscle actin (α-SMA). As shown in **Fig. 3A**, LOX expression was found to be associated with areas of extensive tissue remodeling with the presence of positively birefringent collagen fibers, partially overlapping with extravascular α-SMA-positive cells. Staining with the cardiomyocyte-specific marker cardiac troponin I (cTNI) showed a faint labeling of LOX in cTNI-rich regions around the injured heart, whereas CD45-positive leukocytes seems not to display specific LOX staining **(Supp. Fig. 2)**. The expression of LOX by extravascular α-SMA-positive myofibroblasts was also studied by immunofluorescence. As shown in **Fig. 3B**, positive co-localization of LOX and α-SMA was observed in the injured heart, but we also found a number of LOX-expressing cells that were negative (or very low stained) for α-SMA. Taken together, these results show that LOX family members are highly induced in response to myocardial infarction, presumably contributing to cardiac remodeling by collagen cross-linking, and that myofibroblasts constitute a cell source for the expression of LOX.

TGF-β and hypoxia induce LOX and LOXL expression in cardiac fibroblasts

Next, we investigated whether the induction of LOX genes can be recapitulated in cardiac fibroblasts and analyzed the signal transduction pathways potentially involved. Previous work from different groups including ours has shown that TGF-β and hypoxia are important stimuli

for LOX/L expression in a number of cells and tissues[17-20]. Clinical and experimental evidence point also to a role for TGF-β- and hypoxia-dependent pathways in the heart response to myocardial infarction[21-24]. Accordingly, we found that TGF-β- and hypoxia-dependent pathways were activated in our model of MI as assessed by phospho-Smad and HIF1α staining, respectively **(Fig. 4A and B)**. We then isolated cardiac fibroblasts from mouse ventricles, exposed them under culture conditions to 5 ng/ml of TGF-β1 and hypoxia (1% O_2 tension) or both, and analyzed the expression of LOX/L isoforms. Under our experimental conditions, only TGF-β stimulus was able to promote myofibroblast differentiation, as assessed by α-SMA expression (**Supp. Fig. 3**). As shown in **Fig. 4C**, TGF-β and hypoxia induced the expression of the whole set of LOX isoforms, except for LOXL1 by TGF-β1, as assessed by quantitative RT-PCR. The combination of both stimuli was particularly effective to upregulate the expression of LOX and LOXL2. The induction of the canonical LOX mRNA is followed by protein expression and accumulation in the cell supernatant, as shown in **Fig. 4D and E**. Taken together, these results indicate that the induction of LOX isoforms can be recapitulated *in vitro* by activation of TGF-β- and hypoxia-dependent pathways in cardiac fibroblasts.

LOX activity inhibition improves cardiac function after MI

We show here that LOX/L enzymes are induced as a response to MI at 3-7 days after injury. To determine the role of LOX in heart remodeling following MI, we studied the effect of the inhibition of LOX activity with the small molecule β-aminopropionitrile (BAPN) in the MI mouse model. BAPN (5 mg/kg body weight/day) was administered daily to control animals (sham-operated) and to infarcted mice, starting 8 days after surgery. The extent of collagen content and cross-linking was studied in the scar area by biochemical and histological techniques in the control and BAPN-receiving animals. HPLC-based biochemical evaluation showed a modest though significant increase in the amount of the major stable mature cross-link 28 days post-MI, as represented by hydroxylysylpyridinoline (HP)/triple helix, together with an increase in collagen accumulation, expressed as hydroxyproline/proline ratio **(Fig. 5A and B)**. LOX inhibition with BAPN resulted in a significant reduction in both collagen cross-linking and content. Interestingly, careful analysis under polarized light of the accumulated collagen revealed a diminished presence of orange-red mature collagen bundles in control mice compared to the green-yellow fibers observed in BAPN-treated **(Fig. 5C and D)**. Heart tissue sections stained with Picrosirius red showed a significant reduction in the extent of the fibrotic scar area in BAPN-treated mice 28 days post-MI, as well as a diminished infarct length **(Fig. 5E and F)**. In agreement with these results, BAPN treatment resulted in a reduction in the number of ventricular wall segments with reduced motility as measured by echocardiography, suggesting that BAPN-treated animals have reduced infarct expansion compared to control animals **(Table 1)**. We next analyzed whether BAPN treatment altered the expression of LOX isoforms and certain metalloproteases (MMP) reported to be involved in the heart response to damage [25]. As shown in **Supp. Fig. 4**, except LOXL1 and MMP9, the expression of these matrix remodeling enzymes was found to be upregulated at 28 days post-infarction, and did not change upon BAPN treatment. Interestingly, the expression of the metalloprotease inhibitor TIMP4 was diminished upon MI, and this downregulation was not observed in infarcted mice under BAPN administration.

To assess cardiac function we carried out echocardiographic analysis 3 and 28 days post-injury as well as in uninjured mice. BAPN did not significantly alter cardiac function in control animals **(Table 2)**. However, BAPN administration, starting either 8 days after MI or on the same day of the intervention, reduced ventricular dilatation and improved ejection fraction 28 days post injury, compared to untreated animals. Improved function was accompanied by a reduction in the heart weight/body weight ratio (**Supp. Table. 1**).

Only a few number of molecules have been identified as potential LOX inhibitors (being BAPN the most widely used compound), and even fewer as selectively blocking one particular isoform [26, 27]. To confirm the role of LOX in post-MI cardiac remodeling, we carried out additional experiments using a rabbit polyclonal antibody that blocks canonical LOX activity *in vivo* [28]. As shown in **Fig. 6**, mice subjected to MI and receiving anti-LOX antibody displayed reduced cardiac fibrosis and diminished scar area and infarct size, compared with mice treated with rabbit IgG as a control. Mice treated with anti-LOX antibody displayed significantly reduced ventricular dilatation and improved ejection fraction 28 days post-infarction. This was paralleled by a reduction in the number of ventricular wall segments with reduced motility as measured by echocardiography (**Tables 3 and 4**).

Taken together our results indicate that the inhibition of LOX enzymatic activity, particularly that of the canonical LOX, impairs the formation of a mature collagen matrix upon myocardial infarction, and that this is associated with a beneficial effect on cardiac remodeling and function.

Discussion

The family of LOX enzymes has attracted considerable interest in recent years as their members have been associated with several diseases, particularly in the vascular system and in tumorigenesis[29, 30]. Although biological roles beyond ECM remodeling have been described for LOX members, such as chromatin regulation or cellular chemotaxis, most reported actions in the vascular and cancer settings invoke the capacity of these enzymes to contribute to ECM building and maintenance[29, 31]. In the cardiovascular system, where the ECM plays an essential role in providing the biomechanical properties, pioneering work by Lerman *et al.* reported that LOX activity increased during the healing response to acute myocardial infarction in rabbits [32]. Augmented expression of the canonical LOX has been also reported during the myocardial fibrotic response occurring in spontaneously hypertensive rats (SHR), an observation linked to enhanced collagen cross-linking and deposition[9]. Additional experimental models, such as C57/BL6 mice under a high fat and carbohydrate diet, a model of metabolic syndrome, or rhesus monkeys subjected to left anterior descending artery ligation, developed myocardial fibrosis with increases in collagen cross-linking and LOX activity and/or expression [33, 34]. Clinically, myocardial fibrosis in patients with hypertensive heart disease and chronic heart failure is associated with enhanced LOX expression and matrix cross-linking[9]. These studies investigating the role of LOX in heart diseases were mainly focused on the analysis of the expression of the canonical LOX, with no or very little information on the remaining isoforms. Here we show, to our knowledge for the first time, that the whole set of LOX genes were strongly upregulated in an infarct mouse model. Coordinated expression of all the LOX family members suggests that common signaling pathways are triggered to induce their expression during heart response to injury. TGF-β and hypoxia have been previously shown to be important regulators of the expression of multiple LOX family members in other cell and tissue contexts[18, 20]. Here we also show that, in agreement with previous studies, these signaling pathways were indeed activated after myocardial infarction and promoted the expression of LOX/L in cultured cardiac fibroblasts, the main cell type giving rise to myofibroblasts in the fibrotic heart[21-24]. To this respect, although TGF-β has been described to have a preeminent role in gene expression changes occurring during cardiac fibrosis, tissue hypoxia is a common feature of different conditions leading to cardiac fibrosis, including myocardial infarction and pressure- or volume-overload, and has been reported to induce ECM accumulation and myofibroblast differentiation in cardiac fibroblasts[35-37]. The acquisition of a contractile phenotype by expression of α-SMA is widely used to identify differentiated myofibroblasts [38]. Here we describe that extravascular α-SMA-positive cells constitute a cell source for the expression of the canonical LOX isoform, the most highly upregulated isoform upon myocardial damage[39]. It should be however noted that some cells negative or low stained for α-SMA were also found to contribute to LOX expression. While the nature of these cells is at present unknown, different authors have reported a significant developmental heterogeneity in the origin of cardiac fibroblasts, with the presence of fibroblast cell lineages not expressing α-SMA [40-42]. To make this issue even more complicated, cardiomyocytes have been reported to express LOXL1 upon stimulation with hypertrophic agonists, and T-lymphocytes have been described to regulate cardiac fibroblast LOX expression [43, 44]. In fact, our study also detected upregulation of expression of LOX in cardiomyocytes in the infarcted region; nevertheless this expression was considerably lower than that observed in myofibroblasts.

Deposition and cross-linking of fibrillar collagen during the heart response to damage confers strength that opposes to scar and chamber deformation, but has also a tremendous impact on the mechanical and electrical properties of the myocardium. Antifibrotic and cardioprotective strategies have extensively focused on the attenuation of the fibrotic response [45, 46]. Given that the activation of the TGF-β signaling plays an important role in the initiation and progression

of the fibrotic process, a number of strategies have been established to block or mitigate this signaling pathway in order to reduce cardiac remodeling, unfortunately, without a clear answer. While some studies have reported detrimental effects of TGF-β inhibition in a MI experimental model, other works described that TGF-β signaling blockade by ALK5 inhibition successfully ameliorated myocardial collagen accumulation and cardiac dysfunction [47, 48]. More recently, a small molecule inhibiting ALK5 has been reported to improve cardiac function, and to diminish collagen and collagen cross-linking accumulation [49]. This is in agreement with reports describing the capacity of TGF-β inhibitory peptides to improve cardiac function, in association with reduced collagen cross-linking and LOX expression, in experimental models of pressure overload, though this reflects a distinct clinical condition, presumably being governed by different pathogenetic mechanisms[9]. Whereas there is still some controversy, these findings support TGF-β signaling blockade as an effective therapy to prevent cardiac dysfunction. Nevertheless, their translation to the clinical setting is challenging due to the pleiotropic nature of TGF-β and its modulatory functions of the immune and inflammatory responses. Specific intervention of TGF-β downstream targets contributing to tissue fibrosis might represent more realistic options for the clinical treatment, such as the inhibition of LOX-mediated matrix crosslinking. Using BAPN, it was previously shown that inhibition of LOX enzymatic activity decreased chamber and myocardial stiffness in pigs, therefore proving that these enzymes are important determinants of the biomechanical properties of the intact heart [50]. Upon heart damage, inhibition of LOX activity impaired the accumulation of collagen in a model of cardiac hypertrophy in rats, and more recently, BAPN reduced myocardial fibrosis in a mouse model of aging [51, 52]. While these experiments anticipated the potential use of LOX inhibitors for the treatment of heart disease, the specific contribution of LOX enzymes to cardiac dysfunction in disease models had not been clarified. Here we show that BAPN administration, starting either on the day of the coronary occlusion or 8 days after, reduced the accumulation of mature collagen after chronic MI and this effect was accompanied by reduced ventricular remodeling and improved cardiac function. Although ECM production and maturation is necessary to prevent cardiac rupture after MI, excessive matrix stiffness is associated with increased ventricular dilatation and reduced cardiac function in chronic MI. Based on our observations, LOX enzymes seem to play an important role in the tissue response to damage, and, therefore, LOX inhibitors could be of potential clinical application to treat post-infarction remodeling. Nevertheless, the clinical applicability of LOX inhibition in fibrotic and tumorigenic settings has been seriously questioned due to potential side effects and the lack of selective/specific inhibitors [27]. In this line, BAPN is also referred to be the main factor responsible for osteolathyrism, defined as bone and tissue weakening associated to dietary consumption of seeds of *Lathyrus sativus* or grass pea, this action relying on its capacity to inhibit LOX activity [53]. To this respect, we did not observe in BAPN-treated mice any particular case of cardiac rupture, nor the formation of aortic aneurysms, one of the clinical manifestations described to be associated to LOX inhibition [54]. In fact, human pilot studies using BAPN in specific fibrosis-like pathologies, such as the complications associated to filtration surgery in glaucoma patients [55], have been carried out without serious side effects, and therefore, clinical suitability might be reached if safe dosage and time for treatment parameters are determined. Although decades of research have provided sufficient knowledge to confirm the fundamental role of LOX family members in several pathophysiological scenarios, only a few number of molecules have been characterized as potential LOX inhibitors (being BAPN the most widely used), and even fewer as selectively blocking one particular isoform [26, 27]. Here we show that specific inhibition of the canonical LOX isoform by using a blocking antibody reduced cardiac fibrosis and infarct expansion, leading to a significant improvement in cardiac remodeling and function and suggesting a preeminent role

of this isoform in post-MI remodeling. To this respect, the relevance of this enzyme in cardiac pathophysiology has been recently recognized as the matricellular protein, osteopontin, found to be upregulated during myocardial remodeling in heart failure patients, was reported to promote cardiac fibrosis through activation of the expression and activity of LOX [56].

In conclusion, our results show that LOX family members are highly induced during the response to myocardial infarction and play a significant role in the development of cardiac fibrosis, presumably by activation of TGF-β- and hypoxia-dependent pathways in cardiac fibroblasts. We also show that the interference with the enzymatic activity of LOX proteins, particularly of the canonical LOX isoform, reduces ventricular remodeling and improves cardiac function in a mouse model of MI, and therefore we believe that this family of enzymes may represent a potential therapeutic target in cardiac fibrosis and post-ischemic heart failure. Nevertheless, more research, including the design and development of better inhibitors as well as additional *in vivo* analysis of potential side effects, is demanded in order to consider this family of proteins as a target for clinical intervention.

Sources of funding

This work was supported by grants from Ministerio de Economía y Competitividad (Plan Nacional de I+D+I: SAF2012-34916 to F.R-P., and SAF2012-31451 to E.L-P.), Comunidad Autónoma de Madrid (2010-BMD2321, FIBROTEAM Consortium to F.R-P. and E.L-P.), Fundación Renal "Iñigo Alvárez de Toledo" to F.R-P., and by grants from the European Union's FP7 (ERG-239158, CardioNeT-ITN-289600, CardioNext-ITN-608027) and the Fondo de Investigaciones Sanitarias (RD12/0042/0066) to E.L-P. O.B. is a recipient of a fellowship from the Ministerio de Economía y Competitividad (Formación de Personal Investigador).

Conflict of Interest

None declared.

References

1. van den Borne SWM, Diez J, Blankesteijn WM, Verjans J, Hofstra L, Narula J: Myocardial remodeling after infarction: the role of myofibroblasts, *Nat Rev Cardiol* 2010, **7**:30-37.
2. Weber KT, Janicki JS, Shroff SG, Pick R, Chen RM, Bashey RI: Collagen remodeling of the pressure-overloaded, hypertrophied nonhuman primate myocardium, *Circ Res* 1988, **62**:757-765
3. Thiedemann KU, Holubarsch C, Medugorac I, Jacob R: Connective tissue content and myocardial stiffness in pressure overload hypertrophy. A combined study of morphologic, morphometric, biochemical, and mechanical parameters, *Basic Res Cardiol* 1983, **78**:140-155
4. Kivirikko KI, Myllylä R: Post-Translational Processing of Procollagens, *Ann N Y Acad Sci* 1985, *460*:187-201
5. Trackman PC: Diverse biological functions of extracellular collagen processing enzymes, J Cell Biochem 2005, **96**:927-937
6. Badenhorst D, Maseko M, Tsotetsi OJ, Naidoo A, Brooksbank R, Norton GR, Woodiwiss AJ: Cross-linking influences the impact of quantitative changes in myocardial collagen on cardiac stiffness and remodelling in hypertension in rats, *Cardiovasc Res* 2003, **57**:632-641
7. Norton GR, Tsotetsi J, Trifunovic B, Hartford C, Candy GP, Woodiwiss AJ: Myocardial stiffness is attributed to alterations in cross-linked collagen rather than total collagen or phenotypes in spontaneously hypertensive rats, *Circulation* 1997, **96**:1991-1998
8. Maki JM: Lysyl oxidases in mammalian development and certain pathological conditions, *Histol Histopathol* 2009, **24**:651-660
9. Hermida N, Lopez B, Gonzalez A, Dotor J, Lasarte JJ, Sarobe P, Borras-Cuesta F, Diez J: A synthetic peptide from transforming growth factor-beta1 type III receptor prevents myocardial fibrosis in spontaneously hypertensive rats, *Cardiovasc Res* 2009, *81*:601-609
10. McCormick RJ, Musch TI, Bergman BC, Thomas DP: Regional differences in LV collagen accumulation and mature cross-linking after myocardial infarction in rats, *Am J Physiol.* 1994, **266**:H354-H359
11. Stefanon I, Valero-Munoz M, Fernandes AA, Ribeiro RF, Jr., Rodriguez C, Miana M, Martinez-Gonzalez J, Spalenza JS, Lahera V, Vassallo PF, Cachofeiro V: Left and right ventricle late remodeling following myocardial infarction in rats, *PloS one* 2013, **8**:e64986
12. Felkin LE, Narita T, Germack R, Shintani Y, Takahashi K, Sarathchandra P, Lopez-Olaneta MM, Gomez-Salinero JM, Suzuki K, Barton PJ, Rosenthal N, Lara-Pezzi E: Calcineurin splicing variant calcineurin Abeta1 improves cardiac function after myocardial infarction without inducing hypertrophy, *Circulation* 2011, **123**:2838-2847
13. Erler JT, Bennewith KL, Cox TR, Lang G, Bird D, Koong A, Le QT, Giaccia AJ: Hypoxia-induced lysyl oxidase is a critical mediator of bone marrow cell recruitment to form the premetastatic niche, *Cancer Cell* 2009, **15**:35-44
14. Busnadiego O, Loureiro-Alvarez J, Sandoval P, Lagares D, Dotor J, Perez-Lozano ML, Lopez-Armada MJ, Lamas S, Lopez-Cabrera M, Rodriguez-Pascual F: A pathogenetic role for endothelin-1 in peritoneal dialysis-associated fibrosis, J Am Soc Nephrol 2015, **26**:173-182
15. Wagsater D, Paloschi V, Hanemaaijer R, Hultenby K, Bank RA, Franco-Cereceda A, Lindeman JH, Eriksson P: Impaired collagen biosynthesis and cross-linking in aorta of patients with bicuspid aortic valve, J Am Heart Assoc 2013, **2**:e000034

16. Brand NJ, Lara-Pezzi E, Rosenthal N, Barton PJ: Analysis of cardiac myocyte biology in transgenic mice: a protocol for preparation of neonatal mouse cardiac myocyte cultures, *Methods Mol Biol* 2010, **633:**113-124
17. Busnadiego O, Gonzalez-Santamaria J, Lagares D, Guinea-Viniegra J, Pichol-Thievend C, Muller L, Rodriguez-Pascual F: LOXL4 Is Induced by Transforming Growth Factor beta1 through Smad and JunB/Fra2 and Contributes to Vascular Matrix Remodeling, *Mol Cell Biol* 2013, **33**:2388-2401
18. Sethi A, Mao W, Wordinger RJ, Clark AF: Transforming growth factor-beta induces extracellular matrix protein cross-linking lysyl oxidase (LOX) genes in human trabecular meshwork cells, *Invest Ophthalmol Vis Sci* 2011, **52**:5240-5250
19. Voloshenyuk TG, Landesman ES, Khoutorova E, Hart AD, Gardner JD: Induction of cardiac fibroblast lysyl oxidase by TGF-beta1 requires PI3K/Akt, Smad3, and MAPK signaling, *Cytokine* 2011, **55**:90-97
20. Wong CC, Gilkes DM, Zhang H, Chen J, Wei H, Chaturvedi P, Fraley SI, Wong CM, Khoo US, Ng IO, Wirtz D, Semenza GL: Hypoxia-inducible factor 1 is a master regulator of breast cancer metastatic niche formation, P*roc Natl Acad Sci U S A* 2011, **108**:16369-16374
21. Kido M, Du L, Sullivan CC, Li X, Deutsch R, Jamieson SW, Thistlethwaite PA: Hypoxia-Inducible Factor 1-Alpha Reduces Infarction and Attenuates Progression of Cardiac Dysfunction After Myocardial Infarction in the Mouse, J Am Coll Cardiol 2005, **46**:2116-2124
22. Lee SH, Wolf PL, Escudero R, Deutsch R, Jamieson SW, Thistlethwaite PA: Early expression of angiogenesis factors in acute myocardial ischemia and infarction, *N Engl J Med* 2000, **342**:626-633
23. Edgley AJ, Krum H, Kelly DJ: Targeting fibrosis for the treatment of heart failure: a role for transforming growth factor-beta, *Cardiovasc Ther* 2012, **30**:e30-40
24. Ellmers LJ, Scott NJ, Medicherla S, Pilbrow AP, Bridgman PG, Yandle TG, Richards AM, Protter AA, Cameron VA: Transforming growth factor-beta blockade down-regulates the renin-angiotensin system and modifies cardiac remodeling after myocardial infarction, *Endocrinology* 2008, **149**:5828-5834
25. Lindsey ML, Zamilpa R: Temporal and spatial expression of matrix metalloproteinases and tissue inhibitors of metalloproteinases following myocardial infarction, *Cardiovasc Ther* 2012, **30**:31-41
26. Sampath Narayanan A, Siegel RC, Martin GR: On the inhibition of lysyl oxidase by β-aminopropionitrile, Biochem Biophys Res Commun 1972, **46**:745-751
27. Granchi C, Funaioli T, Erler JT, Giaccia AJ, Macchia M, Minutolo F: Bioreductively activated lysyl oxidase inhibitors against hypoxic tumours, *ChemMedChem* 2009, **4**:1590-1594
28. Erler JT, Bennewith KL, Nicolau M, Dornhofer N, Kong C, Le QT, Chi JT, Jeffrey SS, Giaccia AJ: Lysyl oxidase is essential for hypoxia-induced metastasis, *Nature* 2006, **440**:1222-1226
29. Lopez B, Gonzalez A, Hermida N, Valencia F, de Teresa E, Diez J: Role of lysyl oxidase in myocardial fibrosis: from basic science to clinical aspects, *Am J Physiol Heart Circ Physiol* 2010, **299**:H1-9
30. Mayorca-Guiliani A, Erler JT: The potential for targeting extracellular LOX proteins in human malignancy, *Onco Targets Ther* 2013, **6**:1729-1735
31. Levental KR, Yu H, Kass L, Lakins JN, Egeblad M, Erler JT, Fong SF, Csiszar K, Giaccia A, Weninger W, Yamauchi M, Gasser DL, Weaver VM: Matrix crosslinking forces tumor progression by enhancing integrin signaling, *Cell* 2009, **139**:891-906

32. Lerman RH, Apstein CS, Kagan HM, Osmers EL, Chichester CO, Vogel WM, Connelly CM, Steffee WP: Myocardial healing and repair after experimental infarction in the rabbit, *Circ Res* 1983, **53**:378-388
33. Zibadi S, Vazquez R, Moore D, Larson DF, Watson RR: Myocardial lysyl oxidase regulation of cardiac remodeling in a murine model of diet-induced metabolic syndrome, *Am J Physiol Heart Circ Physiol* 2009, **297**:H976-982
34. Xie Y, Chen J, Han P, Yang P, Hou J, Kang YJ: Immunohistochemical detection of differentially localized up-regulation of lysyl oxidase and down-regulation of matrix metalloproteinase-1 in rhesus monkey model of chronic myocardial infarction, *Exp Biol Med (Maywood)* 2012, **237**:853-859
35. Watson CJ, Collier P, Tea I, Neary R, Watson JA, Robinson C, Phelan D, Ledwidge MT, McDonald KM, McCann A, Sharaf O, Baugh JA: Hypoxia-induced epigenetic modifications are associated with cardiac tissue fibrosis and the development of a myofibroblast-like phenotype, Hum Mol Genet 2014, **23**:2176-2188
36. Tamamori M, Ito H, Hiroe M, Marumo F, Hata RI: Stimulation of collagen synthesis in rat cardiac fibroblasts by exposure to hypoxic culture conditions and suppression of the effect by natriuretic peptides, *Cell Biol Int* 1997, **21**:175-180
37. Dobaczewski M, Chen W, Frangogiannis NG: Transforming growth factor (TGF)-beta signaling in cardiac remodeling, *J Mol Cell Cardiol* 2011, **51**:600-606
38. Chen W, Frangogiannis NG: Fibroblasts in post-infarction inflammation and cardiac repair, Biochim Biophys Acta 2013, **1833**:945-953
39. Daskalopoulos EP, Janssen BJ, Blankesteijn WM: Myofibroblasts in the infarct area: concepts and challenges, *Microsc Microanal* 2012, **18**:35-49
40. Ali SR, Ranjbarvaziri S, Talkhabi M, Zhao P, Subat A, Hojjat A, Kamran P, Müller AMS, Volz KS, Tang Z, Red-Horse K, Ardehali R: Developmental Heterogeneity of Cardiac Fibroblasts Does Not Predict Pathological Proliferation and Activation, *Circ Res* 2014, **115**:625-635
41. Moore-Morris T, Guimaraes-Camboa N, Banerjee I, Zambon AC, Kisseleva T, Velayoudon A, Stallcup WB, Gu Y, Dalton ND, Cedenilla M, Gomez-Amaro R, Zhou B, Brenner DA, Peterson KL, Chen J, Evans SM: Resident fibroblast lineages mediate pressure overload-induced cardiac fibrosis, J Clin Invest 2014, **124**:2921-2934
42. Zeisberg EM, Tarnavski O, Zeisberg M, Dorfman AL, McMullen JR, Gustafsson E, Chandraker A, Yuan X, Pu WT, Roberts AB, Neilson EG, Sayegh MH, Izumo S, Kalluri R: Endothelial-to-mesenchymal transition contributes to cardiac fibrosis, *Nat Med* 2007, **13**:952-961
43. Lucas JA, Zhang Y, Li P, Gong K, Miller AP, Hassan E, Hage F, Xing D, Wells B, Oparil S, Chen Y-F: Inhibition of transforming growth factor-beta signaling induces left ventricular dilation and dysfunction in the pressure-overloaded heart, Am J Physiol Heart Circ Physiol 2010, **298**:H424-H432
44. Ohmura H, Yasukawa H, Minami T, Sugi Y, Oba T, Nagata T, Kyogoku S, Ohshima H, Aoki H, Imaizumi T: Cardiomyocyte-specific transgenic expression of lysyl oxidase-like protein-1 induces cardiac hypertrophy in mice, *Hypertens Res* 2012, **35**:1063-1068
45. Kong P, Christia P, Frangogiannis NG: The pathogenesis of cardiac fibrosis, *Cell Mol Life Sci* 2013, **71**:549-574
46. Weber KT, Sun Y, Bhattacharya SK, Ahokas RA, Gerling IC: Myofibroblast-mediated mechanisms of pathological remodelling of the heart, *Nat Rev Cardiol* 2012, **10**:15-26
47. Frantz S, Hu K, Adamek A, Wolf J, Sallam A, Maier SK, Lonning S, Ling H, Ertl G, Bauersachs J: Transforming growth factor beta inhibition increases mortality and left ventricular dilatation after myocardial infarction, *Basic Res Cardiol* 2008, **103**:485-492

48. Tan SM, Zhang Y, Connelly KA, Gilbert RE, Kelly DJ: Targeted inhibition of activin receptor-like kinase 5 signaling attenuates cardiac dysfunction following myocardial infarction, *Am J Physiol Heart Circ Physiol* 2010, **298**:H1415-1425
49. Engebretsen KV, Skardal K, Bjornstad S, Marstein HS, Skrbic B, Sjaastad I, Christensen G, Bjornstad JL, Tonnessen T: Attenuated development of cardiac fibrosis in left ventricular pressure overload by SM16, an orally active inhibitor of ALK5, *J Mol Cell Cardiol* 2014, **76**:148-157
50. Kato S, Spinale FG, Tanaka R, Johnson W, Cooper Gt, Zile MR: Inhibition of collagen cross-linking: effects on fibrillar collagen and ventricular diastolic function, *Am J Physiol* 1995, **269**:H863-868
51. Bing OH, Fanburg BL, Brooks WW, Matsushita S: The effect of lathyrogen beta-amino proprionitrile (BAPN) on the mechanical properties of experimentally hypertrophied rat cardiac muscle, *Circ Res* 1978, **43**:632-637
52. Rosin NL, Sopel MJ, Falkenham A, Lee TD, Legare JF: Disruption of collagen homeostasis can reverse established age-related myocardial fibrosis, Am J Pathol 2015, **185**:631-642
53. Selye H: Lathyrism, *Revue canadienne de biologie / editee par l'Universite de Montreal* 1957, **16**:1-82
54. Menzies DW, Mills KW: The aortic and skeletal lesions of lathyrism in rats on a diet of sweet pea, *J Pathol Bacteriol* 1957, **73**:223-237
55. Moorhead LC, Smith J, Stewart R, Kimbrough R: Effects of beta-aminopropionitrile after glaucoma filtration surgery: pilot human trial, Ann Ophthalmol 1987, **19**:223-225
56. López B, González A, Lindner D, Westermann D, Ravassa S, Beaumont J, Gallego I, Zudaire A, Brugnolaro C, Querejeta R, Larman M, Tschöpe C, Díez J: Osteopontin-mediated myocardial fibrosis in heart failure: a role for lysyl oxidase? *Cardiovasc Res* 2013, **99**: 111-120
57. Lopez-Olaneta MM, Villalba M, Gomez-Salinero JM, Jimenez-Borreguero LJ, Breckenridge R, Ortiz-Sanchez P, Garcia-Pavia P, Ibanez B, Lara-Pezzi E: Induction of the calcineurin variant CnAbeta1 after myocardial infarction reduces post-infarction ventricular remodelling by promoting infarct vascularization, *Cardiovasc Res* 2014, **102**:396-406

FIGURE LEGENDS

Figure 1. Lysyl oxidase isoforms are induced after myocardial infarction in mice. Time course of collagen accumulation in mice subjected to myocardial infarction as visualized by Picrosirius red staining under brightfield (upper panels) and polarized light (lower panels). **(A)** Representative micrographs and **(B)** analysis of the percentage of heart area occupied by immature (greenish-yellow) and mature (reddish-orange) collagen (left panel) and the fraction of mature collagen (right panel) shown as a function of time (A, B, n=5). **(C)** LOX and LOXL expression was analyzed by quantitative RT-PCR in infarct, border and remote areas (mean ± standard error; n=5, one-way ANOVA followed by Bonferroni's post test, *P<0.05 *versus* no infarction, **P<0.01 *versus* no infarction, dpi: days post-infarction).

Figure 2. Immunohistochemistry of LOX, LOXL2 and LOXL4. Representative micrographs **(A)** and analysis of the percentage of area showing positive immunostaining **(B)** in the infarct scar 7 days after MI (mean ± standard error; unpaired t-test, n=5, *P<0.05 *versus* no infarction, **P<0.01 *versus* no infarction).

Figure 3. Identification of cells expressing LOX in the infarct scar. A) Representative micrographs of consecutive heart tissue sections from control and MI mice (7 days post-infarction) analyzed by immunohistochemistry for the expression of LOX and the myofibroblast marker, α-smooth muscle actin (α-SMA), together with histological staining for collagen accumulation by Picrosirius red (PSR) under brightfield and polarized light. Arrows indicate areas where LOX and extravascular α-SMA expression associates with the presence of positively birefringent collagen fibers. **B)** Representative micrographs of double immunofluorescence of heart sections from control and MI mice (7 days post-infarction) stained for LOX and α-SMA (nuclei with DAPI), and merged images. Under control conditions LOX expression was below detection levels and α-SMA only stained blood vessels. LOX expression was strongly increased upon MI and found to be associated to both α-SMA-positive and negative (or low stained) cells (see arrows). A, B, n=5.

Figure 4. TGF-β and hypoxia induce LOX expression in cardiac fibroblasts. Immunohistochemical analysis of activation of TGF-β and hypoxia-dependent pathways upon myocardial infarction (7 days after MI) in mice as visualized with specific phospho-Smad2 (p-SMAD2) and HIF1α antibodies. **(A)** Representative micrographs from control and infarcted hearts (MI) and **(B)** analysis of percentage of area in the infarct region showing positive immunostaining (mean ± standard error; one-way ANOVA followed by Bonferroni's post test, n=5, *P<0.05 *versus* no infarction, **P<0.01 *versus* no infarction). **(C)** Time course of induction of *Lox/l* mRNA expression by TGF-β 5 ng/ml, hypoxia (1% O_2) or both stimuli simultaneously in cultured cardiac fibroblasts *in vitro* as assessed by quantitative RT-PCR (mean ± standard error; one-way ANOVA followed by Bonferroni's post test, n=6, *P<0.05 *versus* unstimulated, **P<0.01 *versus* unstimulated). **(D, E)** Detection of LOX protein expression in hypoxia- and TGF-β-stimulated cardiac fibroblasts (48 hours of incubation). (**D)** Representative gels assayed for LOX and β-actin (loading control) in total cell extracts (lower panels). Cell supernatants were saved, concentrated and assayed for LOX (upper panel). (**E)** Protein band intensities in cell supernatants (mean ± standard error; one-way ANOVA followed by Bonferroni's post test, n=5, **P<0.01 *versus* unstimulated)

Figure 5. LOX inhibition attenuates cardiac fibrosis. Collagen cross-linking **(A)** and content (**B**) in control and MI mice treated with vehicle or BAPN (starting 8 days after

coronary artery ligation) was measured in the scar area at 28 days post-infarction and expressed as hydroxylysylpyridinoline (HP)/triple helix and hydroxyproline/proline ratio, respectively (mean ± standard error; two-way ANOVA followed by Bonferroni's post test, n=4, *P<0.05 *versus* control, **P<0.01 *versus* control). Collagen staining in heart tissue sections from MI mice under vehicle or BAPN at 28 days post-infarction was visualized by Picrosirius red staining under brightfield and polarized light. **(C)** Representative micrographs, and **(D)** analysis of the percentage of heart area occupied by immature (greenish-yellow) and mature (reddish-orange) collagen (C, D, n=5). **(E)** Representative whole tissue sections from infarcted mice treated with BAPN or vehicle and stained with Picrosirius red. **(F)** Analysis of scar area (percentage of the area occupied by scar) and infarct size (fraction of infarcted left ventricle circumference) (mean ± standard error; unpaired t-test, n=10, **P<0.01 *versus* vehicle).

Figure 6. Selective LOX inhibition ameliorates cardiac fibrosis. Infarcted mice were treated with a neutralizing LOX antibody or control IgG (1 mg/kg body weight/twice weekly), injected intraperitoneally starting eight days after coronary occlusion. Collagen staining in heart tissue sections from mice at 28 days post-infarction was visualized by Picrosirius red staining under brightfield and polarized light. **(A)** Representative micrographs, and **(B)** analysis of the percentage of heart area occupied by immature (greenish-yellow) and mature (reddish-orange) collagen (A, B, n=4). **(C)** Representative whole tissue sections from infarcted mice treated with anti-LOX or control IgG and stained with Picrosirius red. **(D)** Analysis of scar area (percentage of the area occupied by scar) and infarct size (fraction of infarcted left ventricle circumference) (mean ± standard error; unpaired t-test, n=5, **P<0.01 *versus* vehicle).

TABLES

TABLE 1

No MI	**Control**	**BAPN**	
EF (%)	55.20±1.87	52.69±1.57	
LVESV (μl)	33.22±2.49	38.44±2.83	
LVEDV (μl)	74.09±4.21	74.42±3.17	
n	12	10	
3 days post-MI	**Control**	**BAPN d0**	**BAPN d8**
EF (%)	33.67±2.28*	34.51±2.02*	36.04±1.30*
LVESV (μl)	44.70±3.99	45.73±3.29	43.86±2.39
LVEDV (μl)	78.26±5.40	69.48±4.04	68.44±3.20
n	10	14	16
28 days post-MI	**Control**	**BAPN d0**	**BAPN d8**
EF (%)	28.72±2.51*	42.44±2.89*,†,‡	43.79±2.13*,†,‡
ΔEF (pp)	-4.95±2.99	7.93±2.25$^{\#}$	7.75±2.5$^{\#}$
LVESV (μl)	73.29±12.60*,‡	55.18±6.02	43.20±2.85†
LVEDV (μl)	102.34±12.99*,‡	92.35±6.46‡	75.88±2.99†
n	10	14	16

Table 1. Administration of BAPN infarction reduces ventricular dilatation and improves cardiac function after myocardial. Myocardial infarction was induced by ligation of the left coronary artery in male mice and echocardiography analysis was carried out 3 and 28 days later. In the indicated group, BAPN was injected i.p. strating either 8 days post-infarction (d8) or on the day of the surgery (d0). Mean values ±SE are shown. Note that animals used for analysis with no MI are different from those who underwent surgeries. *p<0.05 infarcted vs no MI, †p<0.05 BAPN vs Control, 2-way ANOVA plus Bonferroni post-test. ‡p<0.05 28 days post-MI vs 3 days post-MI repeated-measures 2-way ANOVA plus Bonferroni post-test. #p<0.05 t-test BAPN vs Control. EF, ejection fraction; ΔEF, EF at 28 days minus EF at 3 days; LVESV, left ventricular end systolic volume; LVEDV, left ventricular end diastolic volume; n, number of mice; pp, percentage points.

TABLE 2

LV segment	Control	BAPN d0	BAPN d8
Anterior basal	1.2±0.6	1.0±0.0	1.1±0.3
Anterior mid	2.1±1.0	1.6±0.9	1.4±0.7
Anterior apical	3.4±0.7	2.5±1.0*	1.9±1.0*
Posterior basal	1.0±0.0	1.0±0.0	1.0±0.0
Posterior mid	1.8±0.9	1.2±0.6	1.2±0.4*
Posterior apical	2.9±1.1	1.9±1.0*	1.9±0.7*
n Dysfunctional segments	3.1±1.4	1.9±1.2*	1.8±1.2*
Total score	12.4±3.8	9.3±2.4*	8.4±2.1*
n	10	14	16

Table 2. BAPN reduces infarct expansion and improves cardiac motility after myocardial infarction. Myocardial infarction was induced by ligation of the left coronary artery and echocardiography analysis was carried out 28 days later in the long axis. Where indicated, BAPN was administered to the mice starting either 0 (d0) or 8 days post-MI (d8). Left ventricular wall motility was evaluated by echocardiography in the parasternal long-axis view and scored as follows: 1, normal or hyperkinesis; 2, hypokinesis; 3, akinesis (negligible thickening); 4, dyskinesis (paradoxical systolic motion); 5, aneurysmal (diastolic deformation) [57]. Mean values ±SE are shown for each of the six LV segments. n Dysfunctional segments represents the average number of segments with abnormal motility (infarcted). Total score represents the sum of the score of the six segments. *$p<0.05$ BAPN vs Control (unpaired t-test).

TABLE 3

No MI	**IgG Control**	**Anti-LOX**
EF (%)	50.93±5.15	57.15±4.05
LVESV (μl)	30.68±5.26	21.54±4.70
LVEDV (μl)	61.09±3.84	47.64±6.25
n	5	6
3 days post-MI	**IgG Control**	**Anti-LOX**
EF (%)	31.89±4.25*	30.27±3.77*
LVESV (μl)	46.49±4.58	51.43±3.90*
LVEDV (μl)	68.55±5.96	73.55±2.96*
n	5	5
28 days post-MI	**IgG Control**	**Anti-LOX**
EF (%)	24.71±2.00*	40.88±3.47*,†
ΔEF (pp)	-7.18±3.79	10.61±6.60†
LVESV (μl)	68.73±5.08*,‡	41.81±4.38*
LVEDV (μl)	91.35±6.40*,‡	71.37±7.90*
n	5	5

Table 3. Administration of a neutralizing anti-LOX antibody improves cardiac function after myocardial infarction. Echocardiography analysis was carried out 3 and 28 days after inducing myocardial infarction by ligation of the left coronary artery. Anti-LOX antibody or IgG controls were injected i.p. 3 times a week starting 8 days post-infarction. Mean values ±SE are shown. Note that animals used for analysis with no MI are different from those who underwent surgeries. These uninjured animals were treated with antibodies for 21 days before analysis. *$p<0.05$ infarcted vs no MI, †$p<0.05$ anti-LOX vs IgG Control, 2-way ANOVA plus Bonferroni post-test. ‡$p<0.05$ 28 days post-MI vs 3 days post-MI repeated-measures 2-way ANOVA plus Bonferroni post-test. EF, ejection fraction; ΔEF, EF at 28 days minus EF at 3 days; LVESV, left ventricular end systolic volume; LVEDV, left ventricular end diastolic volume; n, number of mice; pp, percentage points.

TABLE 4

LV segment	IgG Control	anti-LOX
Anterior basal	1.0±0.0	1.0±0.0
Anterior mid	2.4±1.1	1.4±0.6
Anterior apical	4.2±1.1	3.4±1.8
Posterior basal	1.2±0.5	1.0±0.0
Posterior mid	2.4±1.5	1.4±0.6
Posterior apical	3.8±1.1	1.6±0.9*
n Dysfunctional segments	3.8±1.1	2.0±1.2*
Total score	15.0±3.0	9.8±3.0*
n	5	5

Table 4. LOX inhibition reduces infarct expansion and improves cardiac motility of the infarcted heart. Echocardiography analysis in the long axis was carried out 28 days after inducing myocardial infarction by ligation of the left coronary artery. A neutralizing anti-LOX antibody or control IgG were administered i.p. to the mice 3 times a week starting 8 days post-MI. Left ventricular wall motility was evaluated by echocardiography in the parasternal long-axis view and scored as follows: 1, normal or hyperkinesis; 2, hypokinesis; 3, akinesis (negligible thickening); 4, dyskinesis (paradoxical systolic motion); 5, aneurysmal (diastolic deformation) [57]. Mean values ±SE are shown for each of the six LV segments. n Dysfunctional segments represents the average number of segments with abnormal motility. Total score represents the sum of the score of the six segments. *$p<0.05$ anti-LOX vs IgG Control (unpaired t-test).

Figure 1
Click here to download Figure(s): Figure 1.tif

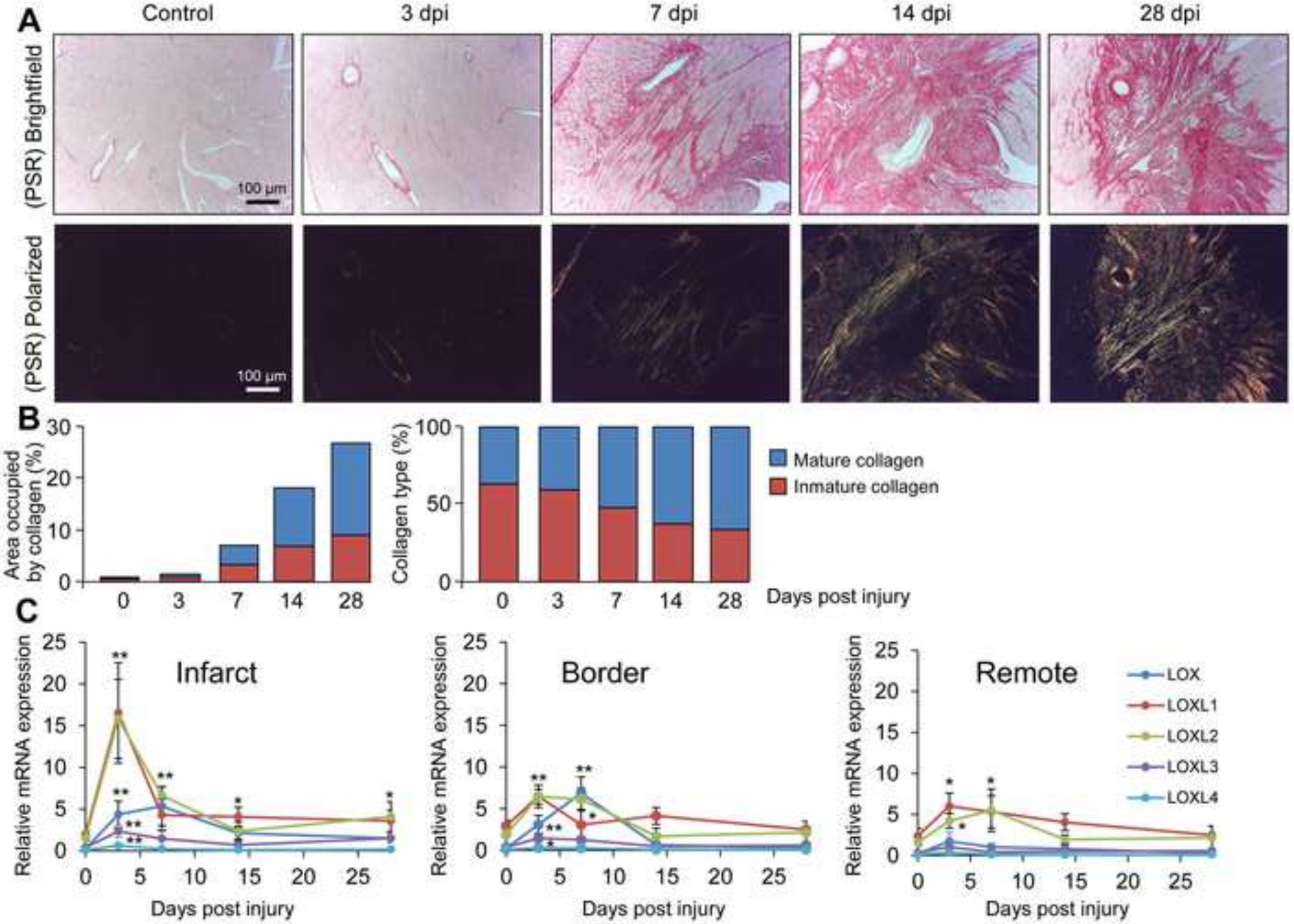

Figure 1

Figure 2
Click here to download Figure(s): Figure 2.tif

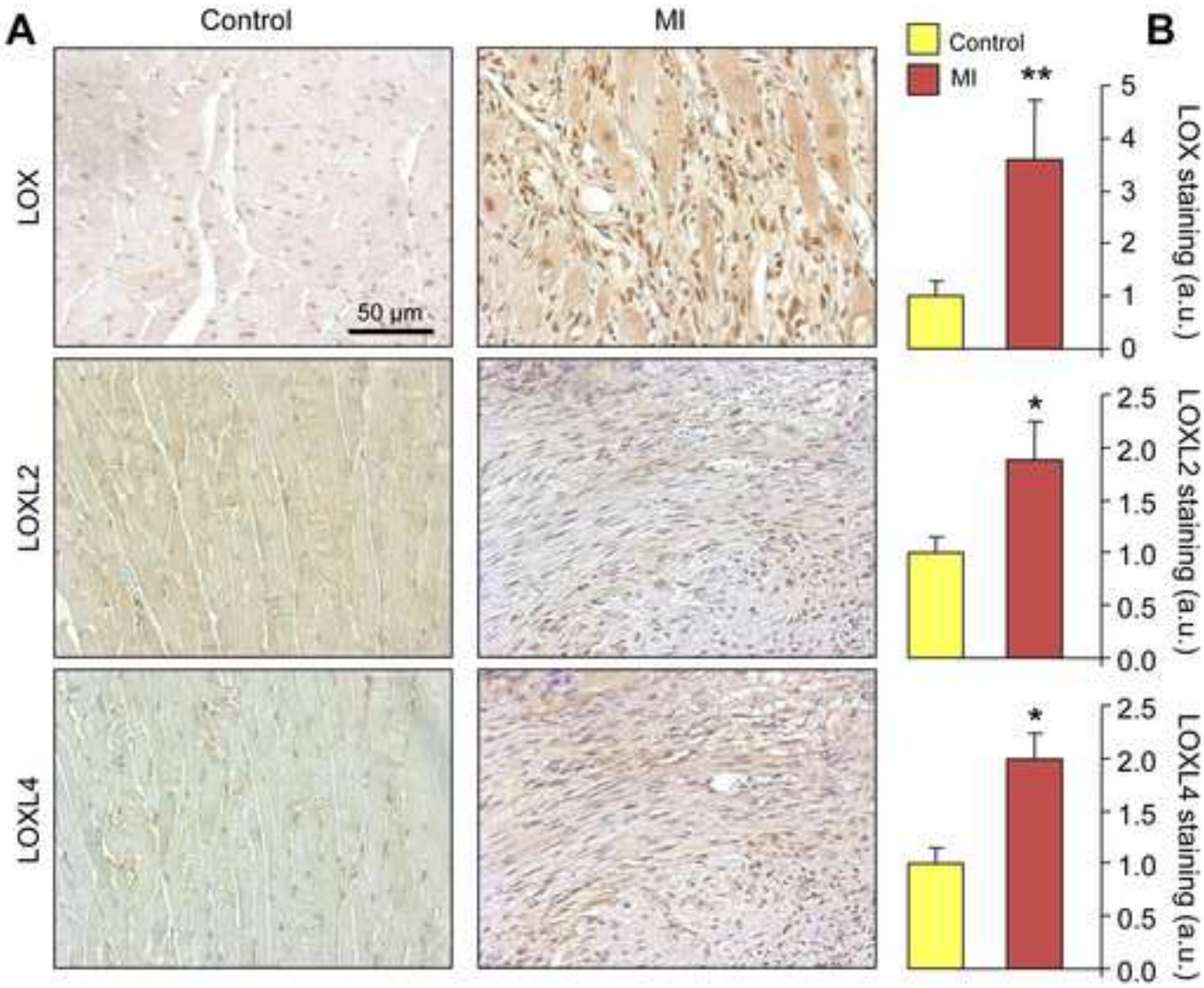

Figure 2

Figure 3
Click here to download Figure(s): Figure 3.tif

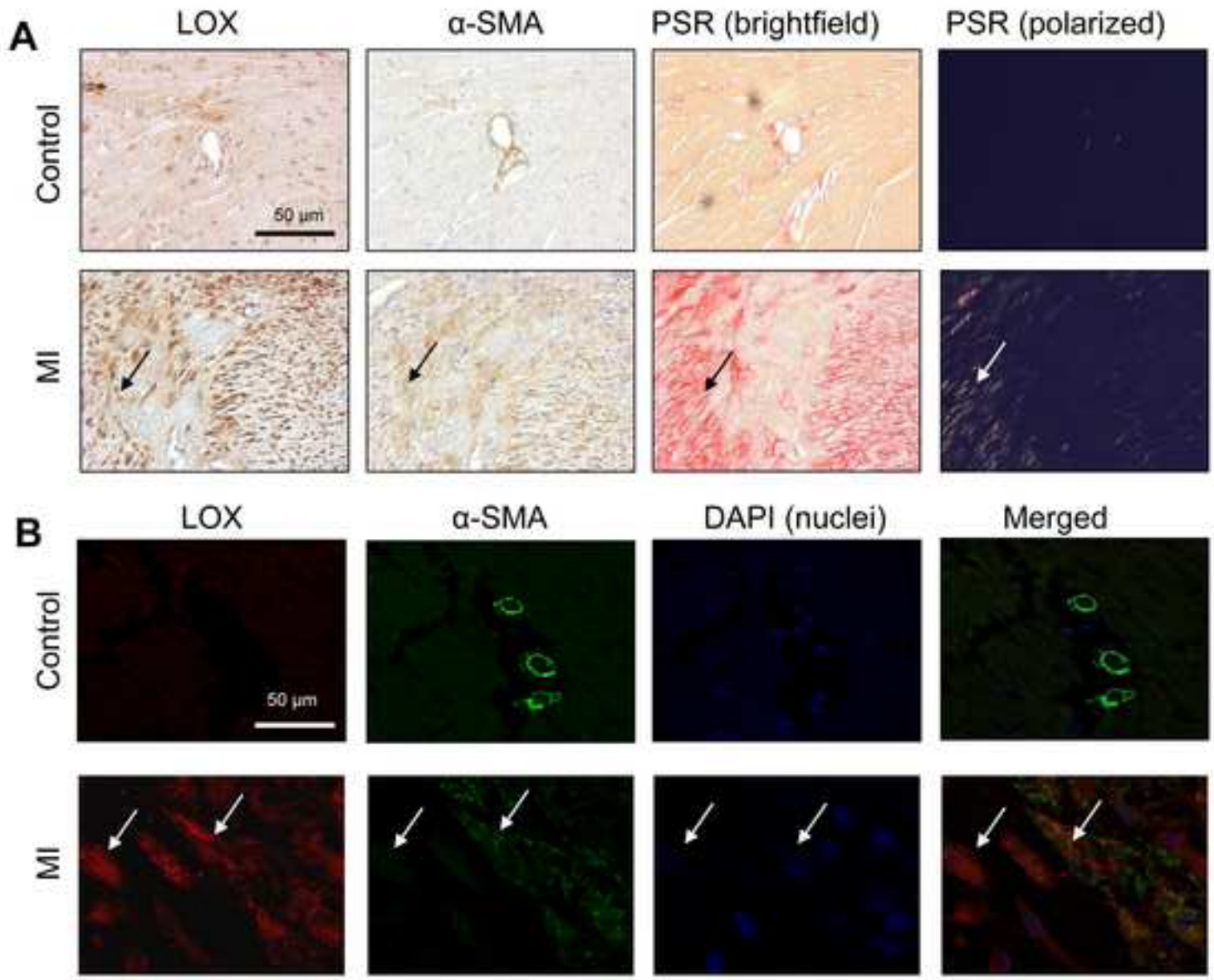

Figure 3

Figure 4

Click here to download Figure(s): Figure 4 new 280715.jpg

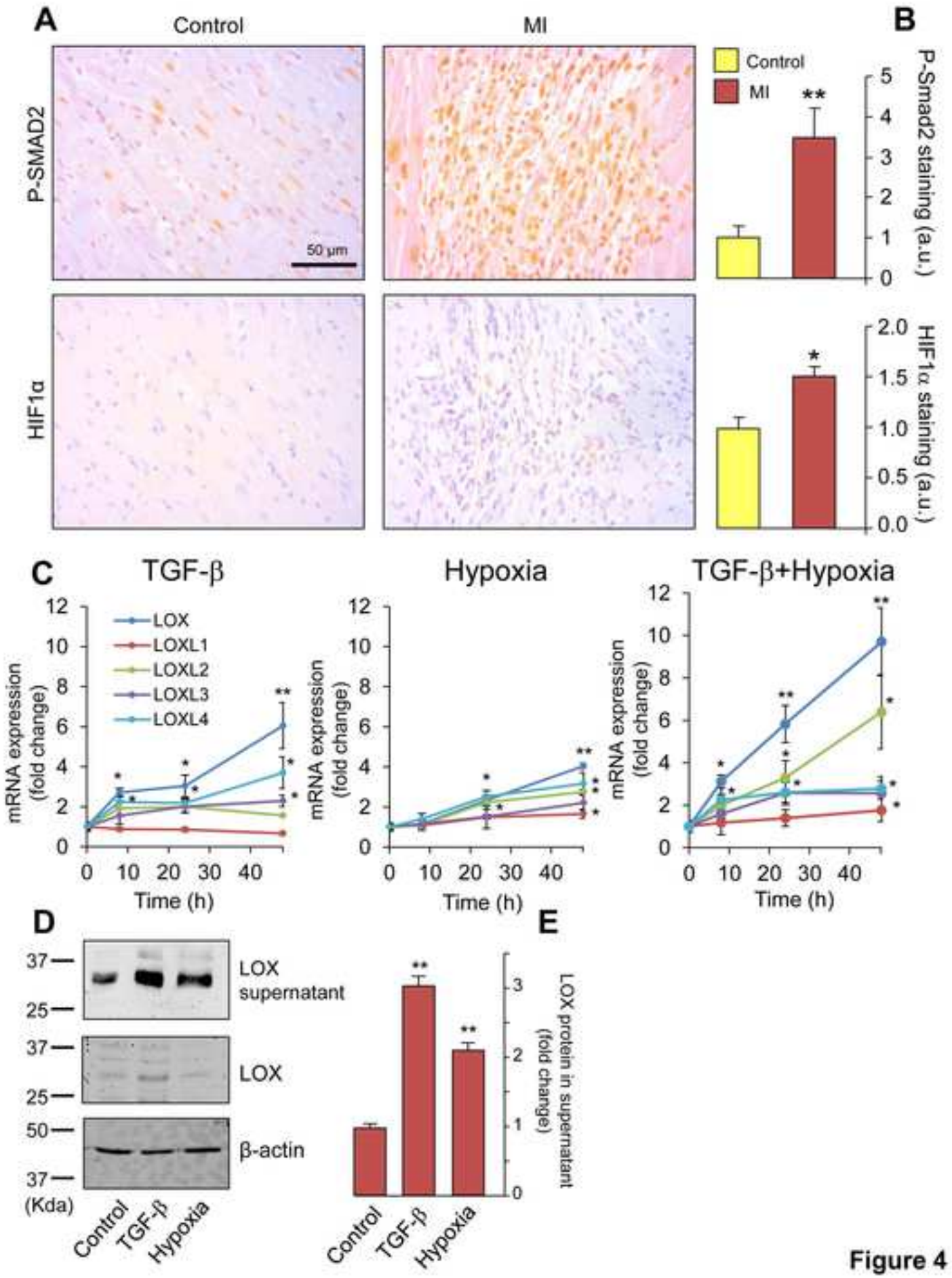

Figure 4

Figure 5
Click here to download Figure(s): Figure 5 new 300715.jpg

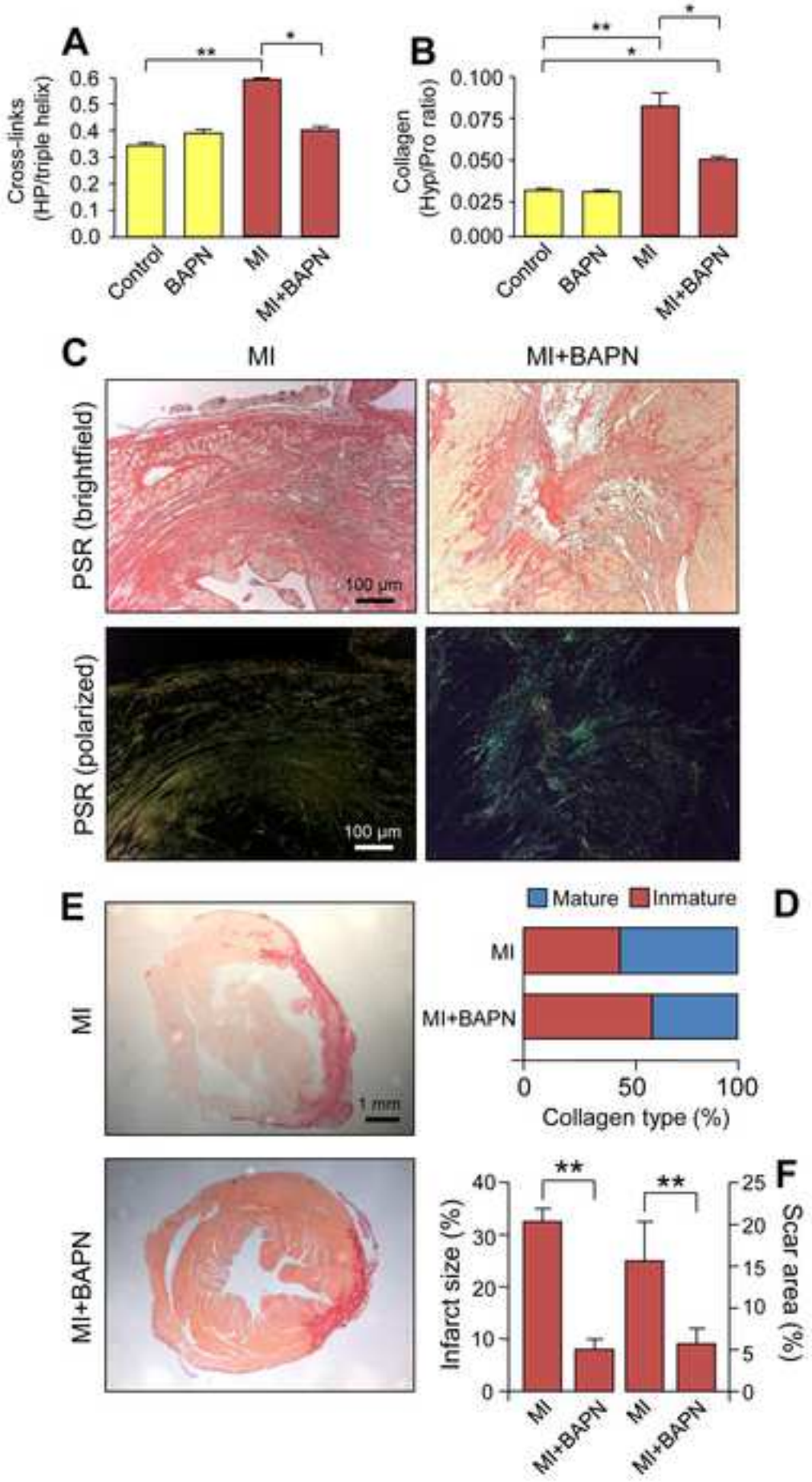

Figure 5

Figure 6
Click here to download Figure(s): Figure 6.tif

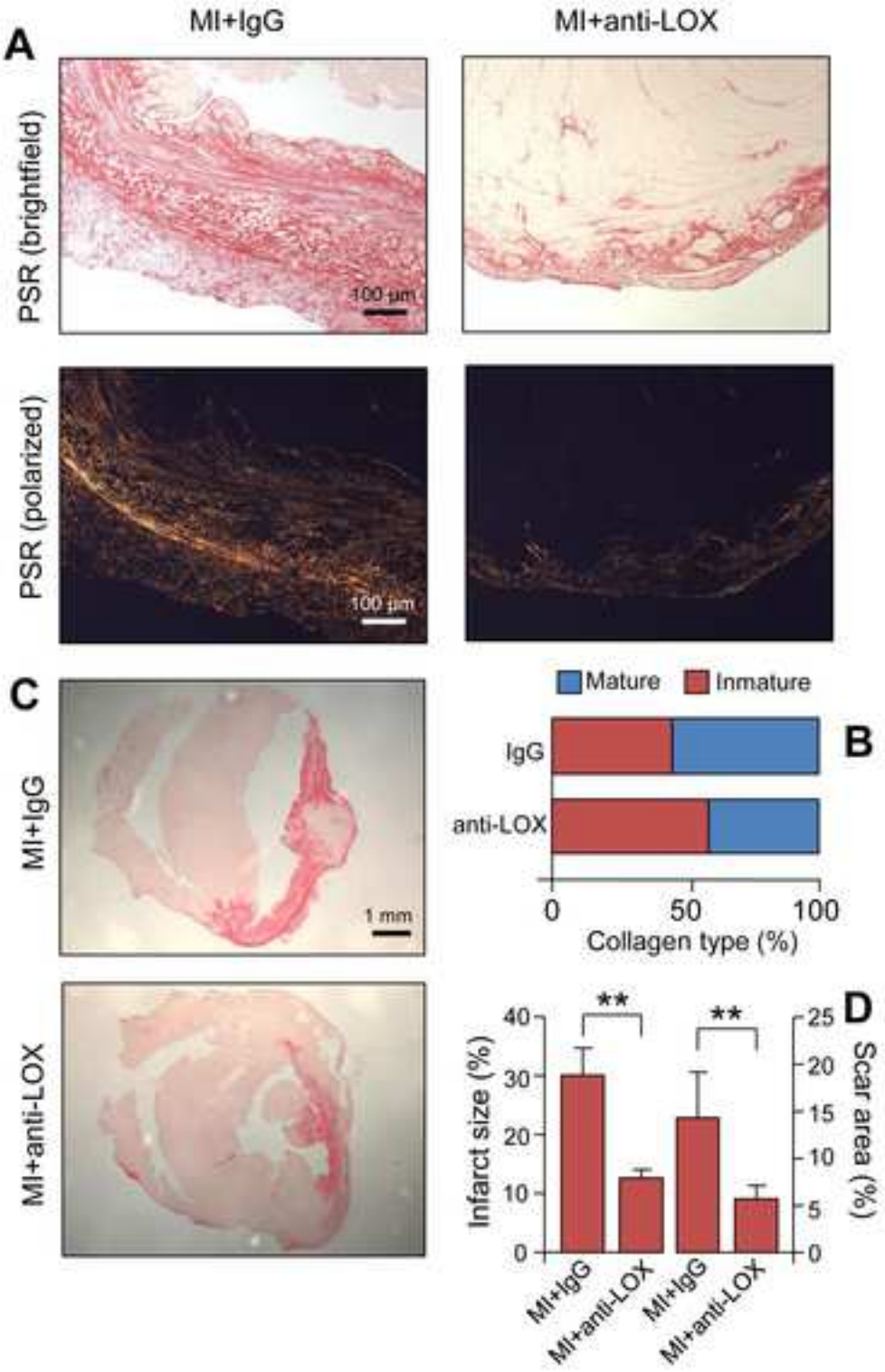

Figure 6

Matrix cross-linking lysyl oxidases are induced in response to myocardial infarction and promote cardiac dysfunction

José González-Santamaría[1], María Villalba[2], Oscar Busnadiego[1], Marina M. López-Olañeta[2], Pilar Sandoval[1], Jessica Snabel[3], Manuel López-Cabrera[1], Janine T. Erler[4], Roeland Hanemaaijer[3], Enrique Lara-Pezzi[2*] and Fernando Rodríguez-Pascual[1*]

[1]Centro de Biología Molecular "Severo Ochoa", Consejo Superior de Investigaciones Científicas (C.S.I.C.), Universidad Autónoma de Madrid (U.A.M.), Madrid, Spain.
[2]Cardiovascular Development and Repair Department, Centro Nacional de Investigaciones Cardiovasculares (C.N.I.C.), Madrid, Spain.
[3]TNO Metabolic Health Research, Leiden, The Netherlands.
[4]Biotech Research & Innovation Centre (BRIC), University of Copenhagen (UCPH), Denmark.

*Enrique Lara-Pezzi and Fernando Rodríguez-Pascual contributed equally to this work.

Online Supplementary Information

Supplemental Methods

Supplemental Figures S1 to S4.

Supplemental Table S1.

Methods

Mice, surgeries and echocardiographic analysis

Myocardial infarction was induced in ten-week-old male C57BL/6 mice (Charles River, Barcelona, Spain) (n=80) by permanently ligating the left coronary artery as previously described[1]. Surgeries were carried out under mechanical ventilation with 3–3.5% sevoflurane. Mice were administered analgesic treatment with buprenorphine (0.3 mg/kg, s.c.) after surgery. The mortality rate in the first 24 h post-infarction was 38%; no mortality was found afterwards. Control, uninfarcted animals were sham-operated.

Cardiac function, chamber dilatation, and wall thickness were analyzed by transthoracic echocardiography 3 and 28 days after infarction, as well as in uninfarcted mice, using a Vevo 2100 high resolution ultrasound system equipped with a 30-MHz linear array transducer (Visualsonics, Toronto, Canada). Measurements were taken by a blinded operator with mice placed on a heating pad under light anaesthesia with isoflurane adjusted to obtain a target heart rate of 500 ± 50 bpm. Continual ECG monitoring was obtained via limb electrodes and synchronized with the ultrasound image. Two-dimensional (2D) and M-mode echocardiography images were recorded in a long and short axis view and the M-mode sample gate was placed at the level of the papillary muscles. Image depth, width and gain were adjusted individually to optimize the image quality and to maintain a frame rate > 200 frames per second.

Echocardiography studies were digitally stored and the analysis was performed off-line (Vevo 2100 Analytic Software). Left ventricular end-systolic volume (LVESV) and left ventricular end-diastolic volume (LVEDV) were measured from 2D parasternal long axis view using bi-plane area–length method and LV ejection fraction (EF) was automatically calculated by the formula ([LVEDV−LVESV]/LVEDV)×100%. The short-axis M-mode images were used to measure left ventricular end-diastolic and end-systolic internal diameter (LVIDd and LVIDs, respectively), left ventricular end-diastolic and end-systolic anterior wall thickness (LVAWd and LVAWs, respectively) and left ventricular diastolic and systolic posterior wall thickness (LVPWd and LVPWs, respectively. Mice presenting an EF above 45% at 3d post-MI were removed from the study. Estimation of infarct size was performed by echocardiography in the paraesternal long axis view. For this purpose, the left ventricle was divided into six different segments (basal, mid and apical, in the anterior and posterior wall) and regional left ventricular function was evaluated in each segment as previous described by the American Society of Echocardiography by a blinded operator (1: normal or hyperkinetic; 2: hypokinetic; 3: akinetic; 4: dyskinetic, paradoxical systolic motion; 5: aneurysmal, diastolic deformation). The number of dysfunctional segments observed and the sum of the individual scores assigned to each of the six segments were employed to estimate the infarct size [2].

For LOX inhibition studies, mice were treated either with β-aminopropionitrile (BAPN, 5 mg/kg body weight/day; Sigma-Aldrich, St. Louis, Missouri) (n=10 per group) or with a rabbit polyclonal antibody reported to specifically block LOX isoform (1 mg/kg body weight/twice weekly), injected intraperitoneally (n=5 per group) [3]. Control mice received PBS as vehicle for BAPN, or the same amount of control IgG (Sigma-Aldrich) for anti-LOX. BAPN treatment started either on the same day or eight days after coronary occlusion. The administration of anti-LOX antibody was initiated eight days after. Both animal trials were ended at day 28 post-infarction. Animals were sacrificed by gradually filling the chamber with carbon dioxide.

All experiments were approved by the local Ethics Committee at the Centro Nacional de Investigaciones Cardiovasculares (PA0410). The investigation conforms to the

principles of Laboratory Animal Care, which are formulated by the National Society for Medical Research and the Guide for the Care and Use of Laboratory Animals (US National Institutes of Health Publication 85-23, 1996), and the Directive 2010/63/EU of the European Parliament on the protection of animals used for scientific purposes.

Histological and immunohistochemical studies

The extent of cardiac damage and fibrosis was assessed by standard histological and immunohistochemical methodologies. Tissue portions were fixed in 4% paraformaldehyde and embedded in paraffin wax for histological and immunohistochemical studies. Cross-sectional 7-μm slices of paraffin-embedded heart tissue were deparaffinized, stained for collagen with Picrosirius red, and counterstained with hematoxylin-eosin using standard protocols. Picrosirius red staining was visualized under brightfield and polarized light using a Nikon Eclipse T2000U (Nikon, Amstelveen, The Netherlands) and a Leica DM LS2 microscope (Leica Microsystems, Solms, Germany). Immunohistochemical stainings were performed to detect LOX, LOXL 1 to 4, α-smooth muscle actin (α-SMA), phospho-Smad2, hypoxia-induced factor 1α (HIF1α), cardiac troponin I (cTNI), and the leukocyte antigen CD45. The following primary antibodies were used: anti-LOX (Ab31238, Abcam, Cambridge, Massachusetts), anti-LOXL1, anti-LOXL2, anti-LOXL3, anti-LOXL4, anti-α-SMA (sc-166632, sc-66950, sc-365286, sc-66952, sc-32251, Santa Cruz Biotechnology, Dallas, Texas), anti-phospho Smad2 (3101, Cell signaling Technology, Beverly, Massachusetts), anti-HIF1α (NB100-105SS, Novus Biologicals, Littleton, Colorado), anti-c-TNI (ab-47003, Abcam, Cambridge, Massachusetts) anti-CD45 (550539, BD Pharmigen, USA). Quantification of stained sections was done by digital image analysis using ImageJ (National Institutes of Health, Bethesda, Maryland) and NIS-Elements software (Nikon). Double immunofluorescence studies with anti-LOX/α-SMA antibodies were done with paraffin-embedded heart tissue sections following protocols previously described [4]. Histological and immunohistochemical studies were done by visualizing at least ten fields of view per section, and blinded analyzed.

Infarct size was histologically quantified from Picrosirius red-stained whole tissue sections by determining the percentage of area occupied by the scar with respect to the total area of the left ventricle; and also by measuring the midline infarct length compared to the whole myocardial midline as previously described [5].

RNA extraction and quantitative real-time reverse-transcribed polymerase chain reaction

For RNA studies, heart tissue was snap-frozen in liquid nitrogen. Total RNA was extracted using the RNAeasy kit (Qiagen), the cDNA was synthesized (iScript cDNA synthesis kit, Bio-Rad, Hercules, California) and quantitative real time reverse-transcribed polymerase chain reaction (RT-PCR) was performed as described with off-the-shelf Taqman probes (Applied Biosystems, Foster City, California) [1]. Analysis was performed with the ΔΔCt method with a GAPDH probe for normalization.

Collagen and collagen cross-linking analysis

Heart tissue portions were hydrolyzed (110°C, 24 hours) in 6 M HCl and collagen (hydroxyproline and proline) and mature trivalent cross-links, hydroxylysylpyridinoline (HP) and lysylpyridinoline (LP), analyzed as described previously[6]. Briefly, the samples were dried and redissolved in 0.4 ml 0.1 M sodium borate buffer (pH 9.5) containing 10

μmol/L pyridoxine (internal standard for the cross-links HP and LP) and 2.4 mM homoarginine (internal standard for amino acids) (Sigma-Aldrich). Samples were diluted 20-fold with 50% (vol/vol) acetic acid (Merck, Darmstadt, Germany) for cross-link analysis. Samples were diluted 250-fold with 0.1 M sodium borate buffer (pH 9.5) for amino acid analysis. Derivatization of the amino acids with o-phtaldialdehyde, iodoacetamide and 9-fluorenylmethyl chloroformate and reversed-phase high-performance liquid chromatography (HPLC) of amino acids and cross-links was performed on a 150 mm×4.6 mm Micropak ODS-80TM column (Tosoh Biosciece) and a partisil 10SCX analytical column (Inacom Instruments), respectively. The amount of collagen is expressed as the hydroxyproline/proline (Hyp/Pro) ratio, and of the cross-link hydroxylysylpyridinoline (HP) as mol HP per mol collagen, assuming 300 hydroxyproline residues per triple helical collagen molecule.

Culture of cardiac fibroblasts

Cardiac fibroblasts were isolated from 8-week old mouse heart tissue using methods previously described [7]. Cells were grown at 37°C and humidified atmosphere of 5% CO_2. The purity of mouse cardiac fibroblasts was determined by the expression of vimentin. Cells were used between 3rd and 6th passages. α-SMA expression was routinely checked by immunoblotting in order to monitor constitutive myofibroblast differentiation. Mouse cardiac fibroblasts were treated for time periods ranging from 8 to 48 hours with TGF-β1 at 5 ng/ml under normoxic or hypoxic conditions (1% O_2 tension, Hypoxystation H35, Don Whitley, Shipley, England). At the end of the experimental period, total RNA or protein were extracted and analyzed following protocols previously described [4]

Statistical Analysis

Data are presented as mean ± SE. In echocardiographic data, the same mice were analysed 3 and 28 days post-infarction, with non-infarcted animals representing a different group of mice. To test for statistical significance, data were analysed by two-way ANOVA followed by Bonferroni post-test for multiple comparisons. In addition, a two-way ANOVA with repeated measures followed by Bonferroni post-test was applied to compare mice at 3 *vs.* 28 days post-infarction. Group differences in quantitative RT-PCR, and histological/immunohistochemical/biochemical quantifications were analysed by one-way ANOVA followed by Bonferroni's post-test. Differences in infarct size by echocardiography were analyzed by unpaired t-test. Statistics was performed with GraphPad Prism 5.0 (La Jolla, California), and differences were considered statistically significant at $P< 0.05$.

References

1. Felkin LE, Narita T, Germack R, Shintani Y, Takahashi K, Sarathchandra P, Lopez-Olaneta MM, Gomez-Salinero JM, Suzuki K, Barton PJ, Rosenthal N, Lara-Pezzi E: Calcineurin splicing variant calcineurin Abeta1 improves cardiac function after myocardial infarction without inducing hypertrophy, *Circulation* 2011, **123**:2838-2847
2. Lopez-Olaneta MM, Villalba M, Gomez-Salinero JM, Jimenez-Borreguero LJ, Breckenridge R, Ortiz-Sanchez P, Garcia-Pavia P, Ibanez B, Lara-Pezzi E: Induction of the calcineurin variant CnAbeta1 after myocardial infarction reduces post-infarction ventricular remodelling by promoting infarct vascularization, *Cardiovasc Res* 2014, **102**:396-406

3. Erler JT, Bennewith KL, Cox TR, Lang G, Bird D, Koong A, Le QT, Giaccia AJ: Hypoxia-induced lysyl oxidase is a critical mediator of bone marrow cell recruitment to form the premetastatic niche, *Cancer Cell* 2009, **15**:35-44
4. Busnadiego O, Loureiro-Alvarez J, Sandoval P, Lagares D, Dotor J, Perez-Lozano ML, Lopez-Armada MJ, Lamas S, Lopez-Cabrera M, Rodriguez-Pascual F: A pathogenetic role for endothelin-1 in peritoneal dialysis-associated fibrosis, J*ournal of the American Society of Nephrology* 2015, **26**:173-182
5. Takagawa J, Zhang Y, Wong ML, Sievers RE, Kapasi NK, Wang Y, Yeghiazarians Y, Lee RJ, Grossman W, Springer ML: Myocardial infarct size measurement in the mouse chronic infarction model: comparison of area- and length-based approaches, *Journal of applied physiology* 1985; 2007, **102**:2104-2111
6. Wagsater D, Paloschi V, Hanemaaijer R, Hultenby K, Bank RA, Franco-Cereceda A, Lindeman JH, Eriksson P: Impaired collagen biosynthesis and cross-linking in aorta of patients with bicuspid aortic valve, *J Am Heart Assoc* 2013, **2**:e000034
7. Brand NJ, Lara-Pezzi E, Rosenthal N, Barton PJ: Analysis of cardiac myocyte biology in transgenic mice: a protocol for preparation of neonatal mouse cardiac myocyte cultures, *Methods Mol Biol* 2010, **633**:113-124

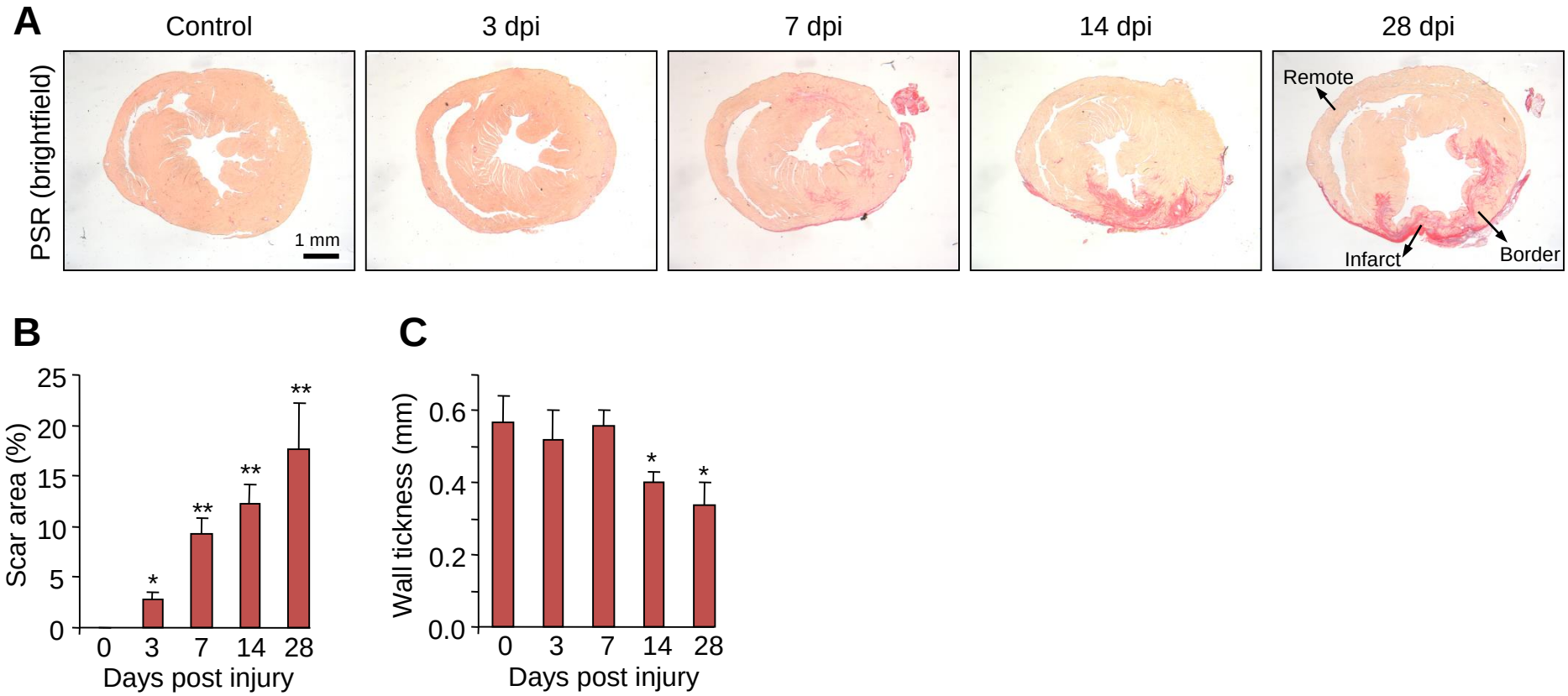

Suppl. Figure 1. Collagen accumulation in a myocardial infarction mouse model. Time course of collagen accumulation in mice subjected to myocardial infarction as visualized by Picrosirius red staining under brightfield. **(A)** Representative micrographs, **(B)** the percentage of area occupied by staining (scar area), and **(C)** the left ventricle wall thickness (in mm) at the site of infarct are shown (mean ± standard error; one-way ANOVA followed by Bonferroni's post test, n = 5, *P<0.05 *versus* no infarction, **P<0.01 *versus* no infarction, dpi: days post infarction).

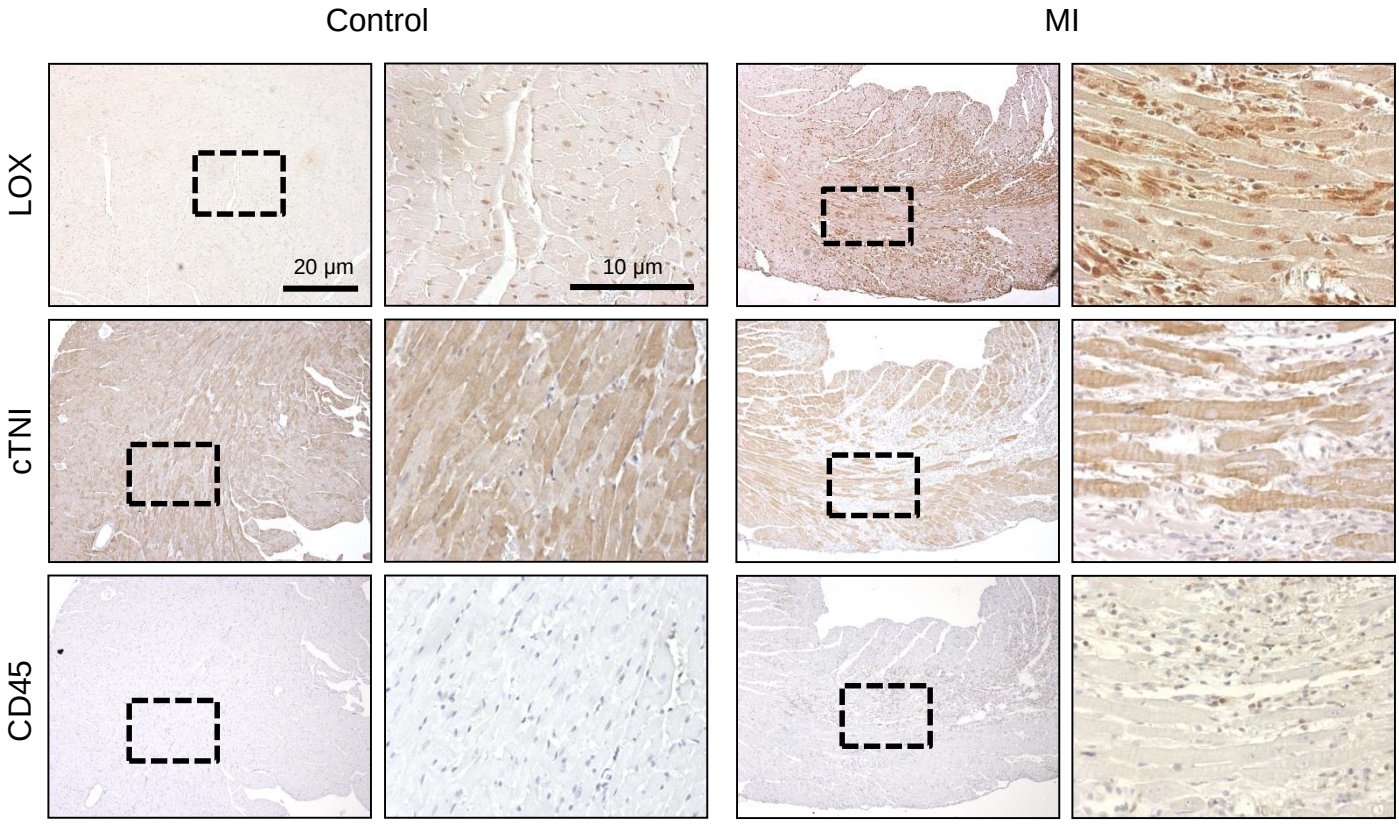

Suppl. Figure 2. Analysis of LOX expression in cardiomyocytes and leukocytes upon MI. Consecutive heart tissue sections from control and MI mice (7 days post-infarction) were analyzed by immunohistochemistry for the expression of the canonical LOX, of the cardiomyocyte-specific marker cardiac troponin I (cTNI), and of the leukocyte marker CD45. Overall LOX staining associated to cTNI-positive cardiomyocytes increased upon injury, indicating that these cells contribute to LOX expression in myocardial infarction, though to a lesser extent than myofibroblasts (see Fig. 3). No specific LOX staining was found in CD45-positive leukocytes.

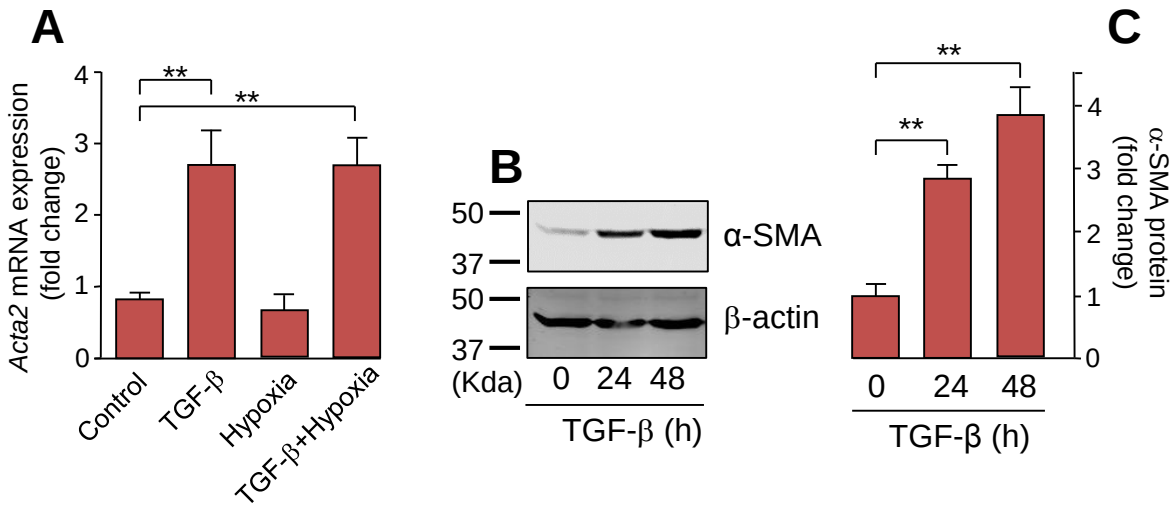

Suppl. Figure 3. Induction of myofibroblast phenotype by TGF-β in cultured cardiac fibroblasts. A) The effect of TGF-β (5 ng/ml), hypoxia (1% O_2), or both stimuli together (48 hours of incubation), on the expression of α-SMA mRNA was determined by quantitative RT-PCR (fold change as mean ± standard error; one-way ANOVA followed by Bonferroni's post test, n=5, *P<0.05 *versus* unstimulated). Time course of α-SMA protein induction by TGF-β analyzed by immunoblotting. **B)** Representative gels assayed with α-SMA and β-actin (loading control) antibodies. **C)** α-SMA protein intensities normalized to β-actin (fold change as mean ± standard error; one-way ANOVA followed by Bonferroni's post test, n =4, **P <0.01 *versus* unstimulated).

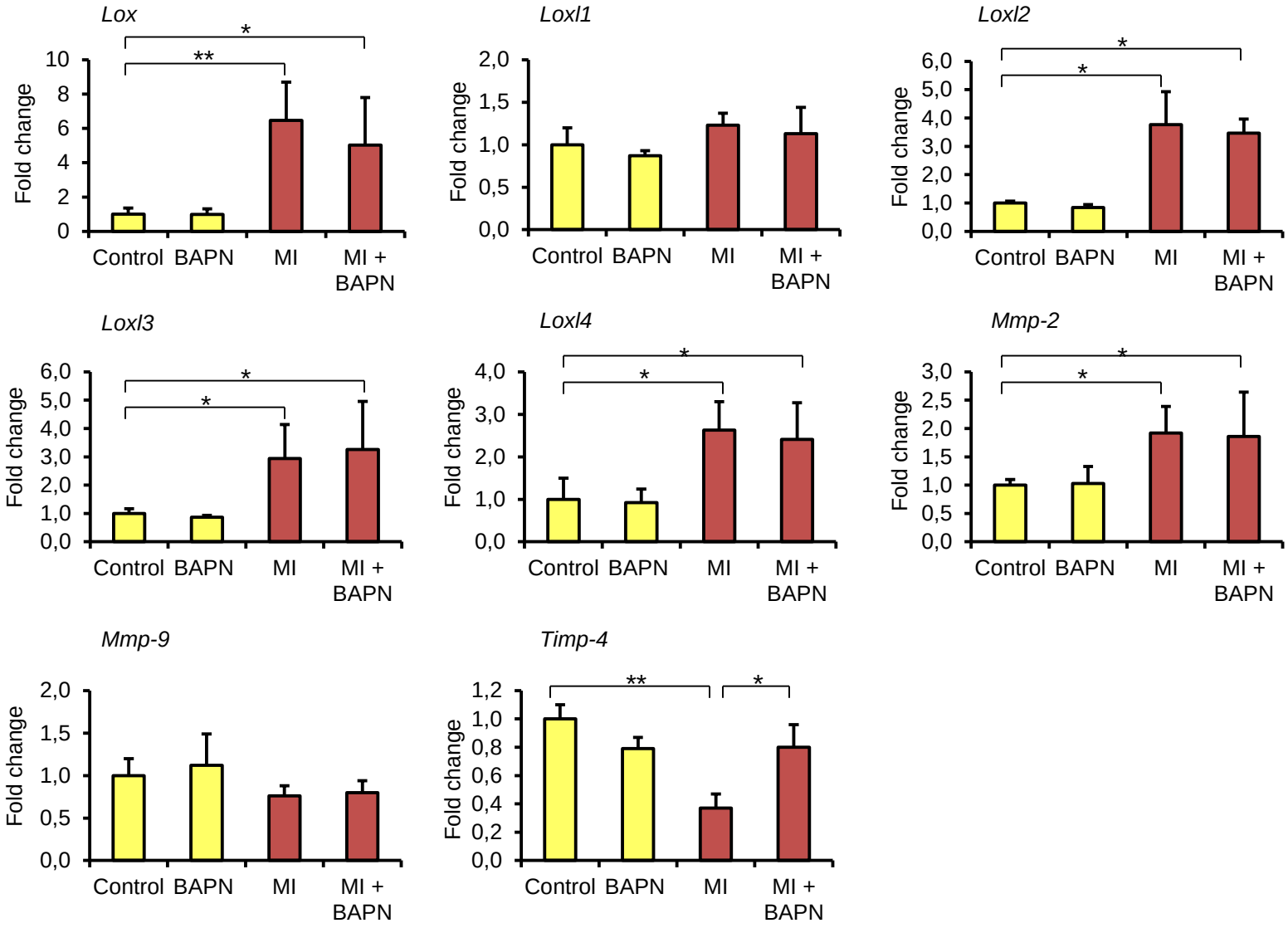

Suppl. Figure 4. Expression levels of LOX isoforms (*Lox and Loxl1-4*), matrix metalloproteases (*Mmp2 and Mmp9*), and its inhibitor *Timp4* in the infarct regions of control and MI mice treated with or without BAPN. mRNA expression was determined by real time quantitative RT-PCR (fold change as mean ± standard error; one-way ANOVA followed by Bonferroni's post test, n=5, *P<0.05 *versus* no infarction, **P<0.01 *versus* no infarction).

SUPPLEMENTAL TABLE 1

No MI	No MI+BAPN	MI	MI+BAPN d0	MI+BAPN d8
5.71±0.18	6.07±0.23	6.51±0.19*	5.81±0.28†	5.92±0.32†

Supplemental Table 1. Administration of BAPN after infarction reduces the hypertrophic response of the heart upon MI. Control and infarcted mice received vehicle or BAPN starting at day 0 (d0) or 8 days after surgery (d8), and were sacrificed 28 days post-infarction. The hypertrophic index was calculated as the heart weight/body weight ratio (*$p<0.05$ infarcted vs no MI, †$p<0.05$ BAPN vs Control, 2-way ANOVA plus Bonferroni post-test.).